IEEE Access
Multidisciplinary | Rapid Review | Open Access Journal

Received 9 June 2024, accepted 29 June 2024, date of publication 3 July 2024, date of current version 12 July 2024.

Digital Object Identifier 10.1109/ACCESS.2024.3422529

STANDARDS

A CQI and Hysteretic-Based Decision Algorithm to Prevent Handover Failures for Pedestrian Mobility in Mobile Communication HetNet

ZHIYI ZHU[1], (Student Member, IEEE), EIJI TAKIMOTO[2], PATRICK FINNERTY[1], (Member, IEEE), AND CHIKARA OHTA[1], (Member, IEEE)
[1]Graduate School of System Informatics, Kobe University, Kobe 657-8501, Japan
[2]Information Technology Center, Nara Women's University, Nara 630-8263, Japan

Corresponding author: Zhiyi Zhu (194x606x@stu.kobe-u.ac.jp)

This work was supported by Japan Society for the Promotion of Science (JSPS) KAKENHI under Grant JP22H03585.

ABSTRACT In current mobile communication networks, handover substantially influences the performance of heterogeneous networks (HetNet). The decision process and trigger timing of the handover decision algorithm (HDA) are integral aspects of handover and are indispensable for mobile user equipment (UE). However, the major A3RSRP (reference signal received power) HDA with the parameter of handover margin (HOM) used in co-frequency environments has poor performance with low-speed pedestrian scenarios in HetNet, including high handover failure (HoF) ratio, frequent handover (FHO), and high number of HoFs. In this paper, we focus on reducing the HoF ratio and propose a novel CQI and hysteretic (CH)-based HDA using downlink channel quality indicator (CQI) and hysteretic control (HC). This novel HDA enables the cell to check the downlink CQI of the UE during HDA, thereby correctly determining the trigger timing of the handover. Moreover, the cell can use the HC to dynamically adjust the HOM based on the CQI of the UE to adapt the handover to the HetNet environment. We evaluate and compare the performance of the CH and A3RSRP HDAs in three scenarios with different speeds, each with multiple HOM settings. The ns-3 simulation results indicate that the CH HDA shows a maximum improvement of 100% in HoF ratio and 5% and 100% in the number of handovers and HoFs, respectively, in the small-scale environment with a speed of 0.5 m/s and an initial HOM of 2.0 dB, while the CH HDA shows a minimum improvement of −4% in HoF ratio and 58% and 44% improvement in the number of handover and HoFs, respectively, in the large-scale environment with a speed of 0.5 m/s and an initial HOM of 3.0 dB, compared with the A3RSRP HDA.

INDEX TERMS A3RSRP, channel quality indicator, handover, handover decision algorithm, handover failure, HetNet, hysteretic control, ns-3.

I. INTRODUCTION

With the rapid evolution of 5G and LTE, numerous small-cells with low output power and small coverage areas have been deployed within a macro-cell of the heterogeneous network (HetNet) to accommodate more communication devices than ever before [1], [2].

Handover is a necessary process for user equipment (UE) to select a cell with the best quality of communication in HetNet. The handover process can be divided into two main parts: handover decision process, also known as HDA, in which the source cell (S-cell) uses measurement reports from UE to determine the timing for the UE to trigger the handover [3], and the handover execution process, wherein the UE sends and receives handover requests between the S-cell and target cell (T-cell), as illustrated in Fig. 1.

In the handover decision process, the UE measurement report includes the reference signal received power (RSRP) and reference signal received quality (RSRQ) from surrounding cells, and the S-cell determines the necessity of a

The associate editor coordinating the review of this manuscript and approving it for publication was Rentao Gu.

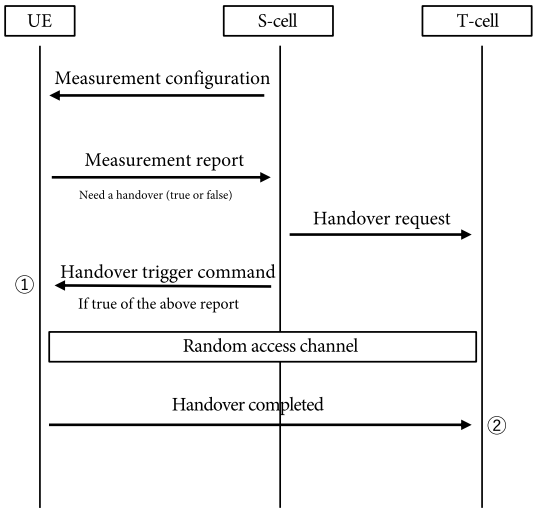

FIGURE 1. Two types of failures in the handover procedure.

handover and to which cell it should be directed based on the received message of the measurement report in Fig. 1.

Generally, the entire handover process proceeds smoothly without handover failure (HoF). However, HoF often occurs when macro-cell and small-cells use the same frequency and are near each other because of the co-frequency interference [3]. According to the specific position of the UE where a radio link failure (RLF) occurs during the message exchange in the handover procedure in Fig. 1, RLF indicates that the UE loses the communication link with the S-cell owing to a poor signal-to-noise ratio (SINR) value [4], [5].

The HoF can be categorized into two main types [6], [7],

- Too-late failure (TLF),
- Too-early failure (TEF).

In a communication environment using the same frequency, the downlink of the UE receives strong co-frequency interference. Consequently, the UE may experience RLF before receiving the handover trigger command [8], which refers to message 1 in Fig. 1. Additionally, because the output power of the small-cell is smaller than that of the macro-cell, sometimes the uplink SINR of the UE degrades to a level where the S-cell cannot receive its measurement report before the UE receives message 1 [3], [8]. As a result, the S-cell cannot receive the measurement report from the UE and cannot send a handover trigger command based on the measurement report, which eventually leads to an RLF of the UE. These two types of HoFs, where the RLF occurs before the UE receives the handover trigger command, are called TLF [5], [9].

Furthermore, the RSRP received by the UE from both the S-cell and T-cell can fluctuate significantly owing to fading, which is a physical phenomenon that occurs during signal propagation. The fading causes the S-cell to receive inaccurate measurement reports from the UE, resulting in the S-cell prematurely determining the UE handover based on the inaccurate RSRP measurement reports from the UE [10]. The measurement report from the UE may not accurately reflect a communication environment, resulting in a poor RSRP of the T-cell [11]. This can cause the T-cell to not receive the handover completion message from the UE, and the message is shown as message 2 in Fig. 1. The HoF where the UE experiences RLF before the T-cell receives message 2 is called TEF [6].

Moreover, the behavior of UEs that repeatedly handovers between the same S-cell and T-cell pair because of the fading communication environment is referred to as frequent handover (FHO) or ping-pong handover (PPHO) [10].

UE in HoF loses its connection to the cellular network, resulting in disconnection and severely degraded quality of service. Frequent handover means that the UE produces multiple unnecessary handovers within a short period, which can lead to extremely unstable communication and even a HoF [4], [12]. Therefore, the HDA must be able to correctly determine the handover trigger timing of the UE [5], [14]. The main A3RSRP HDA used in same frequency networks has two main parameters: handover margin (HOM) and the time-to-trigger (TTT). Although the combination of these two parameters is effective in suppressing TEF and TLF, the HDA is not applicable to all environments. In particular, the shortcomings of the A3RSRP HDA are severe in the HetNet [15], [16], including high HoF ratio, FHO, and a large number of HoFs.

Channel quality indicator (CQI) is used to guide the selection of modulation and coding schemes (MCS) for downlink transmission. Each value of CQI corresponds to an interval of SINR, indicating that despite the fluctuation of SINR, CQI can be maintained as a constant value if the SINR fluctuation is within a certain interval [17]. In other words, the fluctuation of the CQI is slower than the SINR. Meanwhile, the correlation between the fluctuations of the RSRP and SINR in fading environments is consistent [18]. Consequently, the capability of CQI to remain constant and slow fluctuation in a severely fading environment is a valuable property to implement in HDA, with the objective of reducing the high HOF ratio and FHO due to the severely fluctuating RSRP by fading.

On the other hand, hysteretic control (HC) is a control method for power electronic devices that adjusts the switching state of a device based on real-time feedback of the output voltage or current [19]. Consequently, enabling the cell to dynamically adjust the handover parameters setting according to the CQI of the UE using the HC to enhance the performance and robustness of handover is a valuable application due to setting only one HOM parameter is insufficient in a HetNet environment.

In this paper, we propose a novel HDA, CQI+hysteretic (CH), for managing the HDA process through the observation of variations in the downlink CQI of the UE and adjusting the HOM parameter based on the CQI of the UE using HC to reduce the HoF ratio, as well as the absolute number of HoFs and frequent handover.

Based on ns-3 simulation results, the effectiveness of the proposed CH HDA in reducing the HoF ratio, as well as the absolute number of HoFs and frequent handovers, is demonstrated. Therefore, the major contributions of this paper are as follows:

1) A novel HDA, CH-based HDA, based on downlink CQI and HC to improve the existing A3RSRP HDA.
2) Investigation of the effect on the HoF ratio by each 0.5 dB change in the HOM, as well as the change in the number of TEFs and TLFs in the HoF ratio, and an analysis of the reasons for the effect.
3) Reduction in the HoF ratio, as well as the absolute number of HoFs and handovers using CH HDA.
4) A novel interpretation of RSRP and CQI-based at a trigger timing of handover to analyze the occurrence of a HoF.
5) Investigation, using the ns-3 simulation, of the optimal parameter setting in the two HDAs at different movement speeds in the HetNet.

The rest of this paper is organized as follows: Section II discusses the related work on HDA. Section III discusses the HDA scheme of the current A3RSRP HDA. Section IV discusses the proposed CH HDA and its discussion. Section V discusses the differences in performance of the proposed algorithms within the two simulation environments and compares the performance with existing A3RSRP HDAs. In addition, the reasons for the observed differences in the performance by three speeds are discussed. The investigation of the optimal parameter settings for the three speeds in the HetNet is also discussed, as are the trade-off results between the HoF ratio and the handover frequency. Section VI discusses the results based on Section V, and finally, Section VII describes the conclusions and future work.

II. RELATED WORK

A3RSRP HDA involves two main parameters, HOM and TTT, which are crucial for selecting the cell with the best communication quality and resilience against fading. However, the HOM takes precedence over TTT as it determines the timing for a UE to trigger a handover [5], [20]. In addition, the two parameters, HOM and TTT, in the A3RSRP HDA do not dynamically change after a decision [14]. Selecting inappropriate HOM and TTT values because of insufficient knowledge can lead to increased HoF ratio incidents during the handover process. Recognizing the limitations of the A3RSRP HDA, 3GPP Release 8 introduces a self-organizing network entity into the mobile communication network, and this entity enhances handover performance by dynamically adjusting HDA parameters for UE [21]. This strategy, known as mobility robust optimization (MRO) [22], focuses on optimizing HDA.

Subsequent papers concentrated on dynamically adjusting and optimizing the A3RSRP HDA using different measurement indicators to reduce the HoF ratio and the number of frequent handovers. Research on handover can be divided into two main topics: HDA and handover execution. This paper is mainly concerned with HDA. Thus, it focuses on papers related to HDA management and optimization. Furthermore, based on the indicators used in the decision-making process of HDA, the related work is divided into the following two main aspects.

- RSRP/RSRQ based
- SINR based.

RSRP/RSRQ BASED

Reference [23], the author proposed an MRO algorithm to optimize the A3RSRP HDA. Specifically, HoF data were collected based on different failure types in the past time, and the HOM or TTT was dynamically adjusted based on the ratio of a single failure type in the collected HoF. Reference [24], the authors proposed an MRO algorithm to optimize HOM and TTT parameters selection in A3RSRP HDA based on real-time feedback of HoF type, TLF, or TEF, to reduce the FHO. However, the algorithms require the analysis of historical data to adjust the handover parameters, the HOM or TTT. Therefore, the algorithm optimizes handover performance after a certain time by sacrificing historical handover performance.

Reference [25], the author proposed an MRO algorithm based on fuzzy logic control (FLC) to optimize the A3RSRP HDA. This approach considered RSRP, RSRQ, and speed to select better HOM and TTT parameters for the UE based on the changing environment. The results show significant suppression of both the HoF ratio and PPHO. Nevertheless, the authors considered the range of HOM to be insufficient. Furthermore, the HetNet environment was considered in the paper, and the proposed FLC-based approach is generally considered complex and difficult to apply.

Reference [26], the author used a combination of neural networks and FLC to predict the optimal HOM and T-cell prioritization in a 5G environment. The results demonstrated the effectiveness of the approach in optimizing handover success rate and PPHO. Reference [27], the authors used machine learning to optimize the A3RSRP HDA, aiming to determine the optimal HOM and TTT values under a specific network to reduce the HoF ratio and the number of PPHOs. Reference [28], the authors propose an MRO algorithm based on Q-learning to optimize the cell individual offset parameter setting in A3RSRP HDA to reduce the number of PPHOs and HoF ratio within the scenario of random deployment of small-cells. However, such approaches for predicting the optimal parameter setting within the A3RSRP HDA consume substantial computing time and resources, and the algorithm must be retrained after changing the environment, which is good for the specific environment but not for the real-world application.

SINR BASED

Reference [29], the authors proposed a heuristic algorithm to optimize the A3RSRP HDA by considering the SINR, RSRP, RSRQ, and speed. The numerical results showed that the weights of the four components were as follows:

SINR (0.4215), RSRP (0.1054), RSRQ (0.0516), and speed (0.4215). Consequently, in networks with the same frequency, the influence of SINR, RSRP, and speed was high, while the proportion of RSRQ was low when considering measurement indicators. However, the algorithm did not consider the fading environment, potentially leading to an idealized result.

Reference [30], the authors proposed a handover trigger policy based on SINR and the trajectories of moving UE using Markov modeling to enhance the communication capacity of UE in HetNet. The results show that the proposed mathematical model improves the communication capacity by nearly 100% and was very close to the optimal solution. However, the SINR threshold of 1 dB for handover triggering is considered, which indicates that the direction of movement of the UE must have been away from the S-cell. Otherwise, it could result in a TEL.

Reference [31], the author proposed an algorithm based on the SINR and received signal strength to reduce FHO in vertical handover environments and showed that the proposed algorithm was effective.

Moreover, there are some other methods to optimize A3RSRP HDA. Reference [20], the authors propose an approach based on the dwell time of the UE in a cell to reduce FHO by forcing the UE with a short dwell time in a small-cell to hand over to a macro cell. Reference [12], the authors select the optimal small-cell to reduce the HoF ratio and FHO based on the dwell time of the UE in a cell.

Despite the previous works optimizing the performance of the A3RSRP HDA, they focus on the proposal of an MRO algorithm that dynamically adjusts the parameters of the HOM or TTT in A3RSRP HDA using an MRO algorithm for some particular scenarios to reduce the HoF ratio and FHO by using different measurement indicators, such as RSRP, RSRQ, and SINR.

However, all of these works are based on the existing A3RSRP HDA, which indicates the handover trigger conditions in these works are the same as the A3RSRP HDA. Furthermore, since RSRP, RSRQ, and SINR fluctuate drastically in fading environments, resulting in the optimization of A3RSRP HDA parameter settings using RSRP, SINR, and RSRQ usually requires the implementation of FLC, machine learning, or neural networks to accurately predict the optimal HOM or TTT parameter settings for a given environment. However, it is difficult to apply them in LTE and 5G real-world applications because these methods require significant computational time and resources for model learning and training.

III. A3RSRP HANDOVER DECISION ALGORITHM

In handover, there are six measurement events, A1, A2, A3, A4, A5, and A6, used within intra-LTE or intra-5G handover. All events, except for A3 and A6, are triggered based on a comparison with predefined thresholds. In contrast, events A3 and A6 are triggered based on real-time signal quality comparisons between cells. In threshold-based events, the UE triggers event A1 when the signal quality of the serving cell is better than the predefined threshold. Event A2 is triggered by the UE when the signal quality of the S-cell is worse than the predefined threshold. Event A4 is triggered when the signal quality of the T-cell exceeds the predefined threshold. Conversely, event A5 is triggered when the signal quality of the S-cell is worse than the predefined threshold and the signal quality of the T-cell is better than another threshold [2].

Presently, A3RSRP HDA stands as the prevailing algorithm used to determine the trigger timing of UE handover in both LTE and 5G with the same frequency communication environments. The UE triggers a handover based on the satisfaction of a condition known as the "A3 event" which is defined as follows:

$$Mn + Ocn + Ofn > Mp + Ocp + Ofp + A3Offset + Hys, \tag{1}$$

where Mn and Mp are the RSRP of the T-cell and the RSRP of the S-cell, respectively. $A3Offset$ is the offset of the S-cell, and Hys is the RSRP hysteresis parameter by which the T-cell should exceed the S-cell. Ocn and Ocp are cell-individual offsets for the T-cell and S-cell, respectively. Ofn and Ofp are frequency-specific offsets for the T-cell and S-cell, respectively. Since only consider the same frequency (intra-frequency) handover in HetNet, and there is no specific offset for S-cell and T-cell in the paper, we set the Ocn, Ocp, Ofn, and Ofp to zero. Furthermore, $A3Offset$ and Hys are also known as the HOM in the handover. If the (1) is satisfied and continuously satisfied for the TTT time, then the UE is judged to require a handover. To simplify the expression, $A3Offset + Hys$ is defined as $Offset_n$ by [23], and we use the $Offset_n$ notation in the paper later.

IV. CQI+HYSTERETIC HANDOVER DECISION ALGORITHM

CQI is an indicator of the quality of UE communication used in mobile networks, and HC is a commonly used method for controlling the switching of equipment by environmental changes in the world of electrical and electronic engineering. With severe signal fading in the complex communication environments of mobile networks, both RSRP and RSRQ indicators, which are currently widely used in HDA, suffer from severe fading, resulting in poor handover performance. Therefore, in order to address this problem, we consider controlling the HDA process by using a combination of CQI and HC to shift the timing of handover triggering, as detailed in Algorithm 1.

Algorithm 1 shows the conditions and decision process of the proposed CH HDA, where CQI_{avg} denotes the average downlink CQI within 200 ms after rounding. This is because although the downlink CQI fluctuation is slower than SINR and RSRP, the resistance to fading is stronger. However, it is still subject to fading if the CQI is not pre-processed, resulting in the UE sending incorrect measurement reports to the S-cell, as with the RSRP and RSRQ, and we uniformly referred CQI_{avg} to as "CQI" in the following for simplicity of description.

Algorithm 1 CQI+Hysteretic Handover Decision Algorithm

if $CQI_{avg} < T_{\mathrm{CQI}_1}$ and $CQI_{avg} >= 1$ **then**
  if $CQI_{avg} \leq T_{\mathrm{CQI}_2}$ **then**
    $Offset_n = Offset_n - H^-$
  else
    if *Ping-PongHo* **then**
      $Offset_n = Offset_n + H^+$
    else
      $Offset_n =$ initial $Offset_n$
    end if
  end if
  if $Mn > Mp + Offset_n$ **then**
    Wait for TTT to do a handover of the cell
  else if $Mn < Mp + Offset_n$ **then**
    Cancel the handover of the cell
  end if
else
  if $CQI_{avg} >= T_{\mathrm{CQI}_1}$ **then**
    Cancel handover
  end if
end if

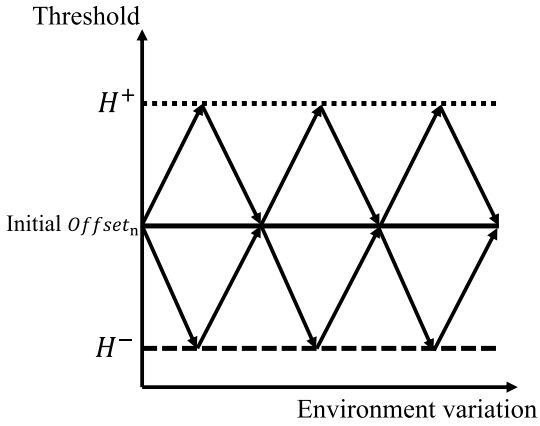

FIGURE 2. The HC scheme considered in the HDA.

Specifically, T_{CQI_1} and T_{CQI_2} are thresholds used to determine UE handover and handover difficulty, respectively, where T_{CQI_1} is used to determine whether handover is necessary for the UE, and T_{CQI_2} is used to determine whether a reduction of the $Offset_n$ is necessary. This reduction is interpreted as a reduction in handover difficulty by the HDA based on the current quality of the communication of the UE.

In HC, there are two parameters, H^- and H^+, which denote the specific value used to determine the decrease of $Offset_n$ according to the CQI and the specific value used to determine the increase of $Offset_n$ according to *Ping-PongHo*, respectively, as shown in Fig. 2. *Ping-PongHo* denotes whether a handover is performed between the same S-cell and T-cell within a short period of time, and if yes, the difficulty of handover is increased by H^+.

Therefore, the whole idea and process of the CH HDA judgment is that it sends a measurement report to the S-cell

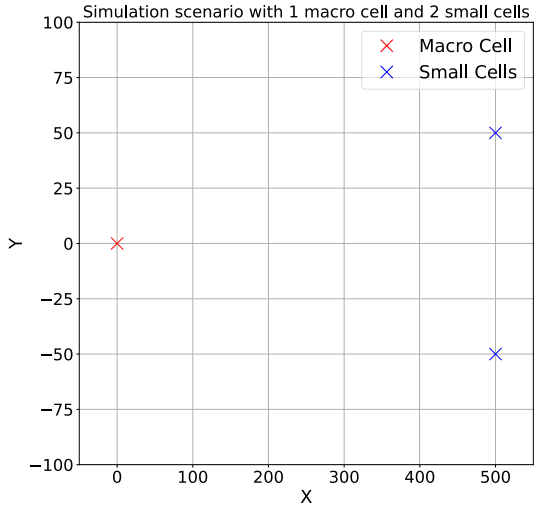

FIGURE 3. Simulation environment with small-scale.

when the UE needs to be handed over. The HDA determines that the current communication environment is degrading and allows the UE to prepare for trigger handover if the CQI of the UE is less than the T_{CQI_1}. Continuously, the HDA determines that the UE must start handover immediately and reduces the decrease the initial $Offset_n$ by H^- if the CQI of the UE is less than T_{CQI_2} before the UE triggers handover. Conversely, the initial $Offset_n$ is maintained if the CQI is not less than T_{CQI_2}. After the UE clears the CQI condition, the CH HDA checks the A3 event described in (1), and the UE will trigger a handover after the TTT time if the A3 event is satisfied while the UE does not trigger the handover and cancels the report of the handover measurement to the S-cell if the A3 event is not satisfied.

Moreover, the handover request of the UE is canceled if the CQI is greater than the T_{CQI_1} before the handover is triggered, regardless of whether the A3 event is satisfied or not.

V. EVALUATION

This paper focuses on the co-frequency HetNet environment, the variation in the number of cells results in the variation in the strength of interference. In addition, as the number of cells varies, the variation in the number of signals received by a UE results in a variation of the fading environment. Therefore, to evaluate the performance of both the proposed CH and the A3RSRP HDAs more comprehensively, we will evaluate the performance of the two HDAs through two simulation environments, which we refer to as small-scale and large-scale environments.

Furthermore, this paper focuses on the triggering conditions and timing of handover and considers ways to improve it. However, other factors often disrupt discussions due to the complex HetNet environment, leading to confusion and marginalization. For example, it is necessary to exclude the HoF owing to factors such as communication congestion or insufficient resource blocks when discussing the triggering

TABLE 1. Simulation parameter setting.

Parameters	Value
Simulation time	1000 s
Frequency	2 GHz
Macro-cell power	46 dBm
Small-cell power	32 dBm
Bandwidth	50 resource blocks
Macro-cell path loss model [10]	$15.3 + 3.76 \times 10\log(R)$, R in m
Small-cell path loss model [10]	$38.46 + 2.0 \times 10\log(R)$, R in m
$Offset_{\mathrm{n}}$	[0.5, 1.0, 1.5, 2.0, 2.5, 3.0] dB
T_{CQI_1}	2, 3, 4
T_{CQI_2}	1, 2
CQI generation interval	1 ms
Hysteretic control (H)	[−1.0, −0.5, 0, 0.5, 1.0] dB
Time interval to judge as a *Ping-PongHo*	1 s
TimeToTrigger	100 ms
Downlink out of synchronization	−5 dB
Timer 310	200 ms
Fading model [3]	Rayleigh fading
Number of UE	5
Low speed [23]	0.5 m/s, 1 m/s, 3 m/s
Mobility model	RandomWalk2dMobility
The number of seeds	5

conditions and handover timing of the A3RSRP HDA and how to improve it. Therefore, in this paper, we consider an environment with a small number of UEs to evaluate the performance of the proposed CH and A3RSRP HDAs.

A. SIMULATION ENVIRONMENT WITH SMALL SCALE

The small-scale environment is illustrated in Fig.3. Specifically, the maco-cell is positioned at the origin (0, 0), and two small-cells using the same frequency with the macro-cell are positioned 500 m away from the macro-cell at (500, 50) and (500, −50), respectively. The performance of the two HDAs is evaluated by the UE moves randomly with the RandomWalk2dMobility model. Furthermore, low-speed UE suffers more severely from fading and is more susceptible to TEF, especially in HetNet [15], [33]. Therefore, this paper considers the scenario of UEs moving at low speed, and the movement of UEs is limited to the range of [200, 500] on the X-axis and the range of [−100, 100] on the Y-axis to limit the UE travel to an irrelevant area with no handover.

Moreover, the parameter $Offset_n$ in the A3RSRP HDA can be selected in the range of [−15, 15] dB. However, the received RSRP from a small-cell by the UE is not expected to be higher than the received RSRP from the macro-cell by the UE 15 dB because the power output of the small-cell is typically low. Similarly, selecting an $Offset_n$ that is too small will increase the number of FHO, owing to the HDA being susceptible to fading, leading to the TEF.

Therefore, we consider $Offset_n$ in the range of [0.5, 3.0] dB, the increment is 0.5 dB, to compare the performance of the CH HDA with the better performance of the A3RSRP HDA, and close to 0.5 dB is considered relatively small $Offset_n$, and close to 3.0 dB is considered relatively large $Offset_n$. Furthermore, only the effect of various $Offset_n$ valves is discussed, the effect of different TTT is not discussed in this paper. Hence, a fixed TTT value of 100 ms is chosen. The specific parameter settings of the simulation environment are shown in Table 1.

B. EVALUATION OF HANDOVER FAILURE RATIO

The baseline for comparison is the $Offset_n$ present in the two HDAs, which have the same value because such a comparison provides a clear view of the effect of our proposed CH HDA on the handover.

Therefore, the two HDAs show the results on HoF ratio when the parameter of $Offset_n$ is set to $Offset_n$ dB in Table 1, for every 0.5 dB interval. Moreover, a handover is not possible with a large value of the CQI. At the same time, a successful handover has a lower probability with a value that is too small, such as the CQI equaling 1. Meanwhile, according to the mapping table of CQI and SINR in [17], a handover is most likely to occur when the SINR changes around 0 dB for the CQI values of 2, 3, and 4. Thus, we choose 2, 3, and 4 as the value of the T_{CQI_1}.

The equation concerning the calculation of HoF is shown as follows:

$$R_{HoF} = \frac{N_{\mathrm{TEF}} + N_{\mathrm{TLF}}}{N_{SUCC\_HO} + N_{\mathrm{TEF}} + N_{\mathrm{TLF}}}, \tag{2}$$

where R_{HoF}, N_{TEF}, N_{TLF}, and N_{SUCC_HO} denote the metric of HoF ratio, the number of TEFs, the number of TLFs, and the number of successful handovers, respectively. The number of handovers is defined as the sum of N_{TEF}, N_{TLF}, and N_{SUCC_HO}. The categorization criteria of N_{TEF} and N_{TLF} are based on Fig.1, which indicates that if message 1 is not received by a UE before an RLF occurs then the number of N_{TLF} is incremented by 1. Similarly, if message 2 is not received by T-cell before an RLF, then the number of N_{TEF} is incremented by 1.

Furthermore, the parameter H of the HC, including the H^+ and H^-, have both positive and negative effects at various UE speeds and combinations. For example, at low speeds of 0.5 m/s, the positive effect of HC is mainly on the H^+, while at relatively higher speeds of 3 m/s, the positive effect of HC is mainly on the H^-. This is because, in the low-speed scenario, the UE's need for handover is extremely low. Hence, increasing the difficulty of handover by the H^+ is beneficial for avoiding the FHO and TEFs and maintaining a stable communication environment. On the other hand, in a higher-speed scenario, the UE's need for handover increases substantially. Consequently, reducing the difficulty of handover by the H^- is beneficial to enable the UE to trigger handover early to reduce the risk of suffering from TLFs or a poor communication environment. Therefore, the parameter combinations for HC with positive effects are prioritized, and for the convenience of the description in the later paper, the parameter H including H^+ and H^- are described as a sum of H^+ and H^-, and the specific H^+ and H^- settings are exhibited in each result.

Regarding the presentation of the simulation results for the HoF ratio in Fig. 4, 6, 8, 11 , 14, and 15. The X-axis

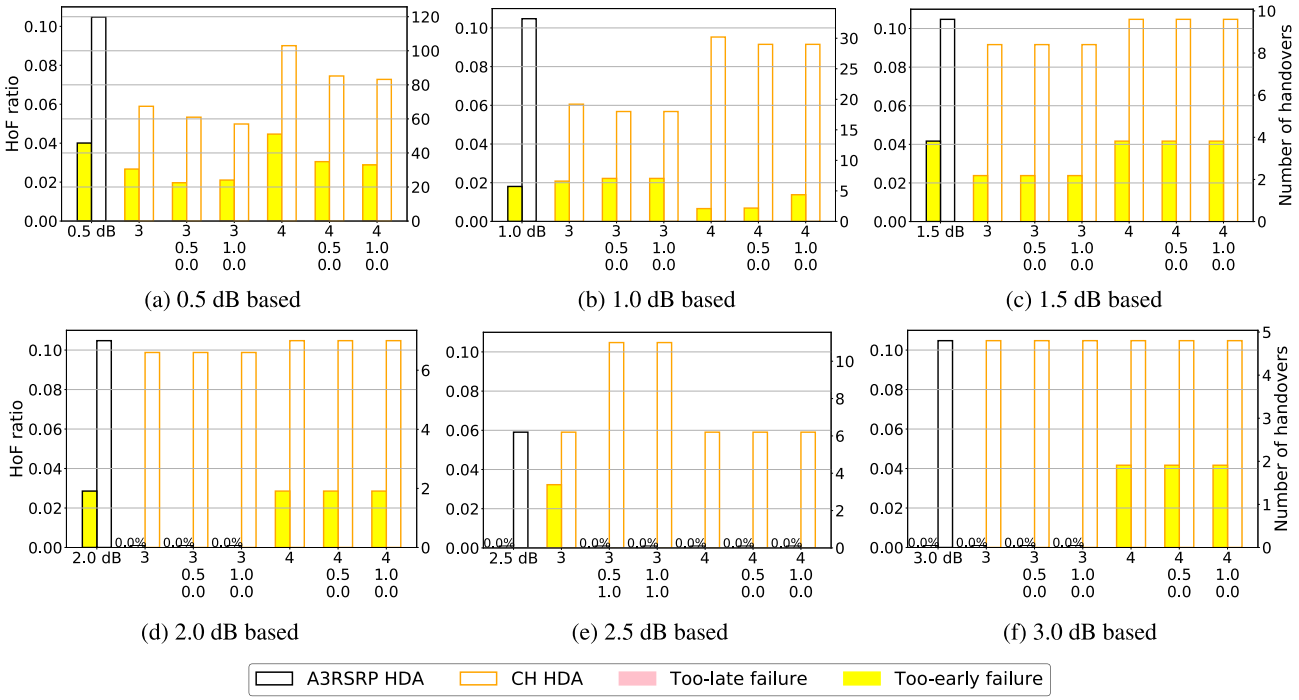

FIGURE 4. Comparison of the HoF ratio and number of handovers for the A3RSRP and CH HDAs at 0.5 m/s speed.

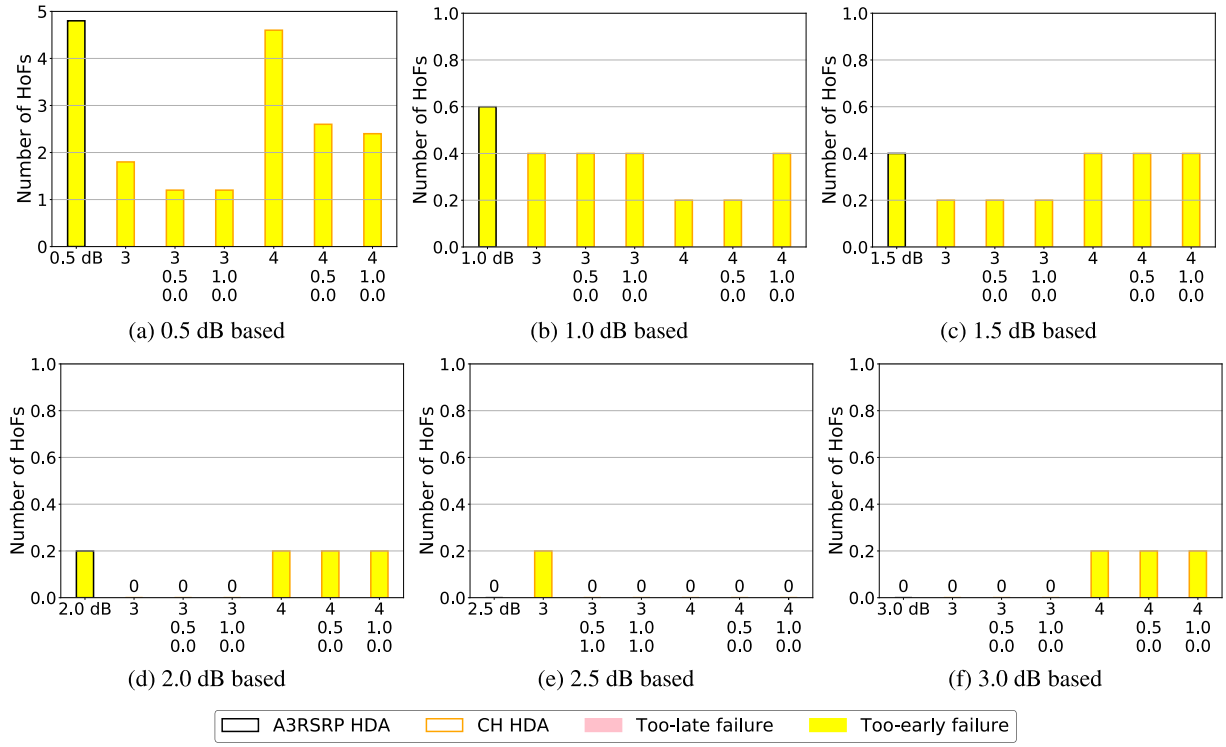

FIGURE 5. Comparison of the number of HoFs for the A3RSRP and CH HDAs at 0.5 m/s speed.

shows parameter settings for the two HDAs, in which the A3RSRP HDA is $Offset_n$ setting, and the CH HDA is T_{CQI_1} threshold and two H parameters settings. For the CH HDA, the upper one is T_{CQI_1}, and below it is the setting of the two H parameters. Furthermore, a dual Y-axis illustrates the HoF ratio and the number of handovers. The left Y-axis

represents the HoF ratio corresponding to the filled histogram on the left side, while the right Y-axis represents the number of handovers corresponding to the empty histogram on the right side. Moreover, Fig. 5, 7, 9 , 12, 14, and 16 shows the performance comparison of the number of HoFs.

1) EVALUATION OF UE MOVING WITH 0.5 M/S

Fig. 4 shows the HoF ratio and number of handovers of both HDAs, and the results are evaluated when the threshold of the T_{CQI_2} is fixed to 1, and UE is moving at a speed of 0.5 m/s.

Fig. 4a shows that the HoF ratio for the A3RSRP HDA is 4%. Since an initial offset threshold of 0.5 dB is selected, a smaller offset threshold results in all HoFs being TEF. Additionally, the results of the number of A3RSRP HDA handovers in Fig. 5a show that when $Offset_n$ is 0.5 dB, although the HoF ratio remains at 4%, resulting in a large number of handovers because a smaller $Offset_n$, which in turn results in a small HoF ratio.

In contrast, the CH HDA decreases the HoF ratio 2% by T_{CQI_1} 3 without HC compared to A3RSRP HDA. The results of the number of handovers for CH HDA in Fig. 5a show that the number of handovers is substantially suppressed by T_{CQI_1} 3 and without HC, and a 43% and 62% reduction in the number of handovers and number of TEFs, respectively, are observed compared to A3RSRP HDA. When T_{CQI_1} 3 with HC, the number of handovers is reduced by 52%, and the number of TEFs is reduced by 75% compared to A3RSRP HDA. When T_{CQI_1} 4 without HC, the suppression of TEFs by CQI is degraded due to the relaxed trigger condition for the CH HDA compared to T_{CQI_1} 3, while the number of handovers is reduced by 14% and the number of TEFs is reduced by 4% compared to A3RSRP HDA. When the T_{CQI_1} is 4 with HC, the number of handovers decreases by 28%, and the number of TEFs decreases by 50% compared to A3RSRP HDA.

Fig. 4b shows that the HoF ratio for A3RSRP HDA is 2%. In contrast, for the CH HDA, the HoF ratio when the T_{CQI_1} is 3 without and with HC is slightly higher than the A3RSRP HDA, while it does not mean that the performance of the CH HDA is worse than the A3RSRP HDA because it decreases the number of handovers and TEFs by 42% and 33%, respectively, when the T_{CQI_1} is 3 without HC compared with the A3RSRP HDA based on Fig. 5a. The number of handovers and TEFs decreases by 45% and 33%, respectively, when the T_{CQI_1} is 3 with HC. Meanwhile, the HoF ratio decreased by 1% when the T_{CQI_1} is 4 without HC, and the number of HoFs is almost negligible. The number of handovers and TEFs decreases by 9% and 66%, respectively, when the T_{CQI_1} is 4 without HC. The HoF ratio decreases by 1%, and the number of handovers and TEFs decreases by 12% and 66% compared with the A3RSRP HDA, respectively, when T_{CQI_1} is 4 with HC and the sum of the H parameter is 0.5 dB. The HoF ratio decreases less than 1%, and the number of handovers and TEFs decreases by 12% and 33%, respectively, when the sum of the H parameters is 1.0 dB. The performance when the sum of the H parameter is 1.0 dB is worse than the sum of the H parameter is 0.5 dB because the timing of the handover trigger is excessively shifted backward, resulting in a slightly increased number of TEFs. Thus, inhibiting a handover by shifting the trigger timing of the handover backward significantly may cause the UE to undergo uncertain fading after the handover is triggered, resulting in low SINR and a TEF. As we described in Fig. 1, the T-cell cannot receive message 2, leading to a TEF.

Fig. 4c shows that the HoF ratio is 4% when the initial $Offset_n$ is 1.5 dB. In contrast, the CH HDA reduces the HoF ratio by 2% when the T_{CQI_1} is 3 with HC. Moreover, the number of handovers and TEFs decreases by 12% and 50%, respectively, when the T_{CQI_1} is 3 with and without HC compared with the A3RSRP HDA based on the result in Fig. 5c, because the effect of suppressing handovers and TEFs mainly dominated by the T_{CQI_1}, and a T_{CQI_1} taking 3 shift the trigger timing of the handover backward as we described in Fig. 4b, In addition, the HoF ratio when the T_{CQI_1} is 4 with or without HC is the same as the A3RSRP HDA. This is because most FHO has been suppressed, and the remaining handovers are difficult to eliminate by a T_{CQI_1} of 4 based on the initial $Offset_n$ value at 1.5 dB.

Fig. 4d shows that the HoF ratio of the A3RSRP HDA is about 3%. In contrast, the CH HDA reaches zero HoF when the T_{CQI_1} is 3, which means no failure in all the handovers, and the same zero HoF is also achieved when HC is considered based on the result in Fig. 5d. Moreover, the number of handovers decreases by 5% based on the result in Fig. 5d. The number of TEFs reaches zero when the T_{CQI_1} is 3 with and without HC, which decreases the number of TEFs by 100% compared with the A3RSRP HDA. In addition, the results of the T_{CQI_1} 4 are almost the same with A3RSRP HDA, this is the same as the result in Fig. 4c.

Fig. 4e shows that zero HoF is also achieved for the A3RSRP HDA when the initial $Offset_n$ is 2.5 dB. This result shows that the initial $Offset_n$ should be at least 2.5 dB for the A3RSRP HDA to suppress most of the TEFs and handovers owing to the fading. In contrast, the HoF ratio of CH HDA is 3%, and while the number of handovers is the same with the A3RSRP HDA when the T_{CQI_1} is 3 without HC, the CH HDA causes slight TEFs. This worse result is because the triggering timing of the handover is shifted backward too much owing to the T_{CQI_1} of 3 and a large value of the initial $Offset_n$, which may cause the UE to undergo uncertain fading after the handover is triggered and result in poor SINR even TEF. Meanwhile, zero HoF is achieved regardless of whether the sum of the H parameters is -0.5 dB or 0 dB when the T_{CQI_1} is 3 with HC while the number of handovers increases by 77% compared with the A3RSRP HDA based on the result in Fig. 5e. This is because when T_{CQI_1} 3 and large $Offset_n$, it is necessary to set the sum of the H to zero or negative in order to neutralize significantly shifted backward timing of the handover. However, the negative sum of the H will increase the number of handovers. In addition, the result of T_{CQI_1} 4 is the same with the A3RSRP HDA. This is because T_{CQI_1} 3 is not as effective as T_{CQI_1} 3 in suppressing handover

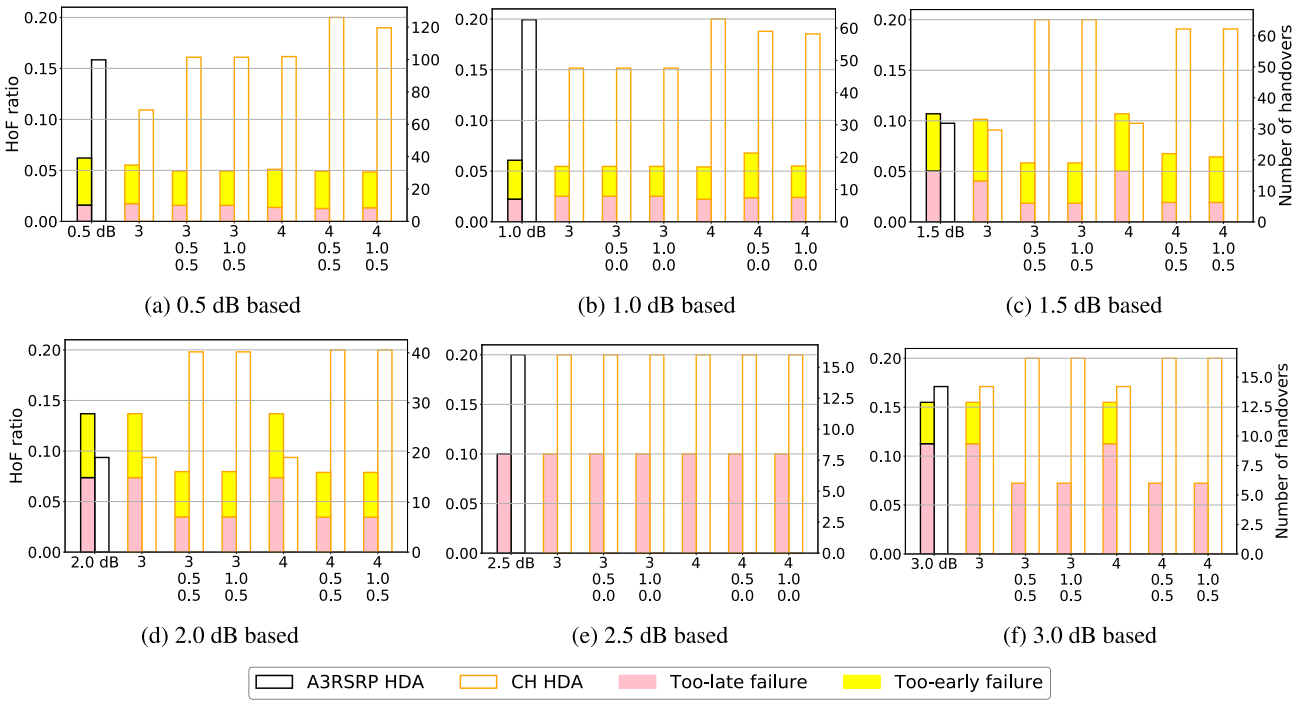

FIGURE 6. Comparison of the HoF ratio and number of handovers for the A3RSRP and CH HDAs at 1 m/s speed.

and TEF, and A3RSRP HDA has the suppression effect on FHO and TEF for 0.5 m/s low-speed scenario when the initial $Offset_n$ at least 2.5 dB.

Fig. 4f shows that the A3RSRP HDA still achieves zero HoF when the initial $Offset_n$ is considered 3.0 dB. In contrast, the CH HDA also achieves zero HoF when the T_{CQI_1} is 3 with and without HC. Furthermore, the number of handovers by the T_{CQI_1} values of 3 and 4 is the same as the A3RSRP HDA, but some TEFs occur when the T_{CQI_1} is 4. This is because the handover trigger timing of shifted backward by the T_{CQI_1} 4 is worse compared to the T_{CQI_1} 3 for a scenario with a low-speed movement of 0.5 m/s and an initial $Offset_n$ of 3 dB. Therefore, it is suggested to choose the CH HDA with a combination of T_{CQI_1} 3 and HC in a low-speed scenario, and it is not suggested to choose the CH HDA with a combination of T_{CQI_1} 4 and HC in a low-speed scenario.

2) EVALUATION OF UE MOVING WITH 1 M/S

Fig. 6 shows the HoF ratio and number of handovers of the CH and A3RSRP HDAs at a speed of 1 m/s, and the threshold of the T_{CQI_2} is fixed to 2.

Regardless of how the parameters are adjusted by the two HDAs, zero HoF cannot be achieved, and TLFs occur. As the moving speed of UE increases, the received RSRP from the cells is subjected to more severe fading compared with those at 0.5 m/s moving speed in the same time period. These results are the same with [10], [12], and [15], where a severe delay in handover triggering due to the setting of an unsuitable handover threshold will lead to severe degradation of the communication quality of UE, which results in a TLF.

Meanwhile, the co-frequency interference causes the downlink SINR of the UE to be low, leading to decoding failures and packet loss, which results in a TLF independent of speed. Therefore, with the increasing speed of movement, the UE exhibits more serious TLFs compared with the scenario of 0.5 m/s.

Fig. 6a shows that the HoF ratio for the A3RSRP HDA is 6% when the initial $Offset_n$ is 0.5 dB. More than half of the HoFs are TEFs, and the remainder are TLFs due to the selection of a small $Offset_n$. In contrast, the HoF ratio of CH HDA decreases by 1% when the T_{CQI_1} is 3 without HC compared with the A3RSRP HDA.

Moreover, the CH HDA reduces the number of handovers, TLFs, and TEFs by 31%, 33%, and 40%, respectively, when T_{CQI_1} 3 without HC compared to the A3RSRP HDA based on Fig. 7a. This reason is the same as the result we described in Fig. 4. The CH HDA decreases the number of TLFs and TEFs by 11% and 22%, respectively, while increasing the number of handovers by 1% when the T_{CQI_1} is 3 with HC compared with the A3RSRP HDA. This is because after considering HC and the sum of H parameters is 0 dB and 0.5 dB, the CH HDA increases the $Offset_n$ to increase the difficulty of handover triggering to reduce TEFs and decreases the $Offset_n$ to decrease the difficulty of handover triggering to reduce TLFs by the HC. However, the decreased difficulty of the handover rigger by the H^- in the H has resulted in a slight increase in the number of handovers. Meanwhile, the CH HDA reduces the number of TLFs and TEFs by 11% and 18%, respectively, while the number of handovers increases by 2% compared with the A3RSRP HDA when

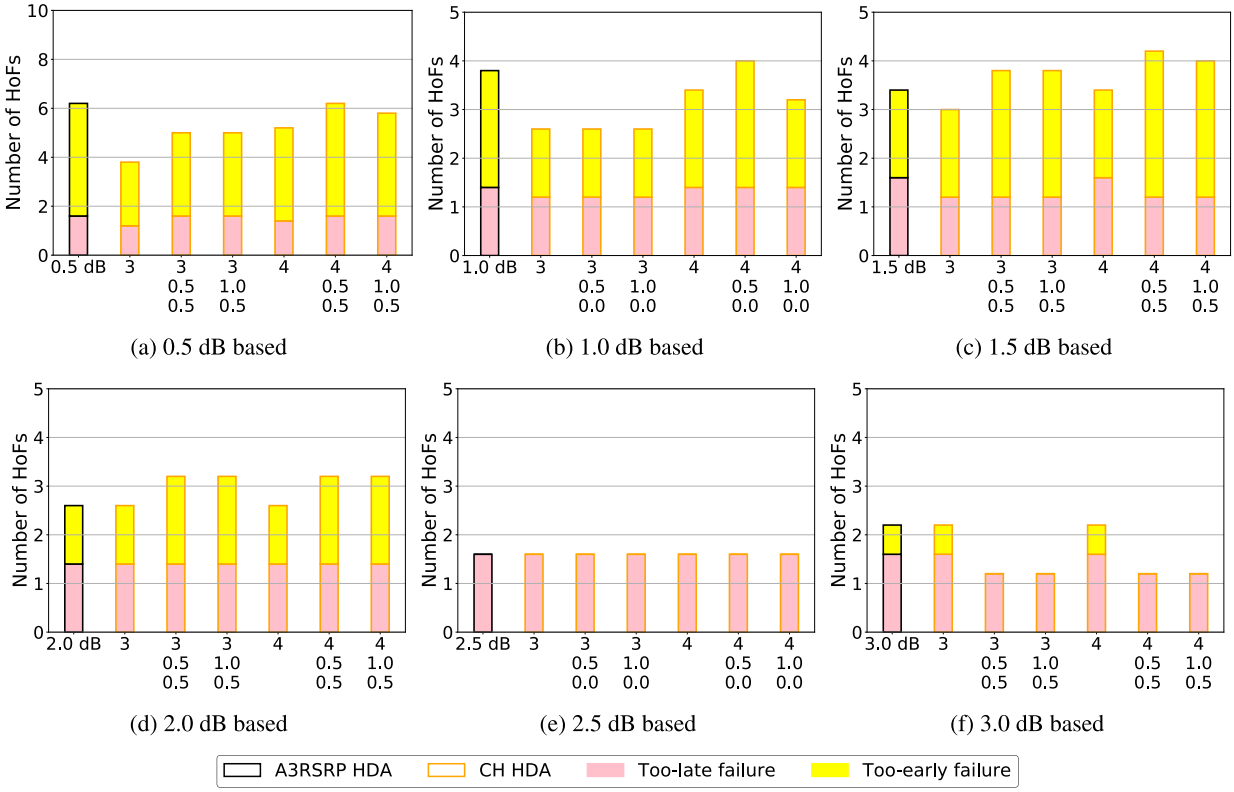

FIGURE 7. Comparison of the number of HoFs for the A3RSRP and CH HDAs at 1 m/s speed.

T_{CQI_1} 4 without HC. When T_{CQI_1} is 4 with HC, the number of TLFs and TEFs are reduced by 0% and 9%, respectively, while the number of handovers increases by 26% and 19%, respectively. This is because the suppresses effect of the sum of H 0.5 dB on the TEFs is more than when the 0 dB, but both include H^-. Thus, the number of handovers increases in order to reduce the number of HoFs. From this result, it can be seen that the effectiveness of suppressing TEF with a T_{CQI_1} 4 can be enhanced by the HC.

Fig. 6b shows that the HoF ratio for A3RSRP HDA is 6%. In contrast, the HoF ratio of the CH HDA reduces by 1% compared with A3RSRPHDA when T_{CQI_1} is 3 with or without HC. The HoF ratios of CH HDA decrease by 1% when T_{CQI_1} is 4 without HC compared with A3RSRP HDA, while the HoF ratios of CH HDA increase by 1% and decrease by 1% when the sum of the H is 0.5 dB and 1.0 dB, respectively.

Moreover, the number of handovers, TLFs, and TEFs are reduced by 24%, 25%, and 36%, respectively, compared with the A3RSRP HDA when T_{CQI_1} is 3 with or without HC based on the result in Fig. 7b. Meanwhile, the number of TEFs is reduced by 18% with almost the same number of handovers, while the number of TLFs is the same as A3RSRP HDA when T_{CQI_1} is 4 without HC compared with the A3RSRP HDA. Although the number of handovers decreases by 5%, the number of TLFs remains the same and the number of TEFs increases by 9% compared with the A3RSRP HDA when T_{CQI_1} is 4 with HC and the sum of H is 0.5 dB. When T_{CQI_1} is 4 with HC and the sum of H parameters is 1.0 dB, the number of handovers, TLFs, and TEFs decrease by 7%, 12%, and 18%, respectively, compared with A3RSRP HDA. This reason is the result in Fig. 4f.

Fig. 6c shows that the HoF ratio for the A3RSRP HDA is 11%. In contrast, the CH HDA reduces the HoF ratio by 1% when T_{CQI_1} is 3 without HC and by 5% when HC is considered, while the HoF ratio is the same when T_{CQI_1} is 4 without HC, and the HoF ratio reduces by 5% when HC is considered.

Moreover, the CH HDA reduces the number of handovers and TLFs by 7% and 25%, respectively, the number of TEFs remains unchanged when T_{CQI_1} is 3 without HC, reducing the number of TLFs by 25% when the T_{CQI_1} is 3 with HC, while increases the number of handovers and TEFs by 105% and 44% compared with the A3RSRP HDA when the sum of the H is 0 dB and 1.0 dB based on the result in Fig. 7c. Despite the CH HDA increasing the number of handovers when the T_{CQI_1} 3 with HC compared with the A3RSRP HDA, T_{CQI_1} can correctly determine the timing of the handover trigger and hence reduces the HoF ratio by 5% without increasing an excessive number of TEFs. Meanwhile, the number of handovers, TLFs, and TEFs does not change when the T_{CQI_1} is 4 without HC compared with the A3RSRP HDA because the effect of T_{CQI_1} 4 on suppressing handover and HoFs is still weaker than T_{CQI_1} 3. The CH HDA reduces the number

of TLFs by 12% and increases the number of handovers by 95% when the T_{CQI_1} is 4 with HC, in which the number of TEFs increases 55% and 44% by the sum of H 0 dB and 0.5 dB, respectively. Regardless of the T_{CQI_1} 3 or 4, the H^- dominates in the HC to reduce the number of TLFs that stand the majority in the HoF ratio, which makes the handover easier to trigger, increasing the number of handovers and TEFs.

Fig. 6d shows that the HoF ratio for the A3RSRP HDA is 13%. In contrast, the CH HDA reduces the HoF ratio by 5% when T_{CQI_1} is 3 and 4 when HC is considered, while the HoF ratio of the CH HDA is the same as the A3RSRP HDA when HC is not considered. Moreover, the number of handovers, TLFs, and TEFs are the same as that of A3RSRP HDA when T_{CQI_1} is 3 and without HC based on the result in Fig. 7d. This is because there are few number HoFs when the initial $Offset_n$ is raised to 2.0 dB, and the number of handovers by the A3RSRP HDA has been substantially suppressed, which makes it difficult to further improve the HoF ratio by the CH HDA with the current parameters combination. Meanwhile, the CH HDA reduces the HoF ratio by 5% when the T_{CQI_1} is 3 and 4 and HC is considered, although the number of handovers and TEFs increase by 110% and 50%, and the number of TLFs is the same as that of the A3RSRP HDA, which implies that CH HDA can maintain a higher handover success rate by correctly determine the timing of handover trigger without substantially increase in the number of HoFs.

Fig. 6e shows that the HoF ratio of A3RSRP HDA is 10%, and only the TLFs can be observed. This indicates that most of the TEF caused by fading can be avoided in the case of A3RSRP by an initial $Offset_n$ of 2.5 dB. Therefore, this parameter is optimal for A3RSRP HDA in this movement scenario. In contrast, the CH HDA exhibits the same as the A3RSRP HDA with and without HC when the T_{CQI_1} is 3 and 4 based on the results in Fig. 6e and Fig. 7e. This is because the current initial $Offset_n$ is the optimal parameter setting under this scenario. Therefore, it is not recommended to use the H^- in HC to reduce the number of TLFs based on this $Offset_n$, since additional TEFs may be induced.

Fig. 6f shows that the HoF ratio for the A3RSRP HDA is 15%. In contrast, the CH HDA reduces the HoF ratio by 7% when T_{CQI_1} 3 and 4 with HC compared with the A3RSRP and reduces the number of TEFs by 100%, achieving zero TEF, while the HoF ratio of the CH HDA is the same as the A3RSRP HDA when the T_{CQI_1} is 3 and 4 without HC. Moreover, the number of TLFs and TEFs decreased by 25% and 100%, respectively, while the number of handovers increased by 16% when the T_{CQI_1} is 3 and 4 with HC, and the result of the CH HDA is the same as A3RSRP HDA when there is no HC compared with the A3RSRP HDA based on the result in Fig. 7f. This is because CH HDA performance can still be maintained well by correctly determining the trigger timing of the handover in the case where $Offset_n$ continues to increase from 2.5 dB, while the performance of A3RSRP HDA degrades obviously.

Based on the comparison results of Fig. 6 and Fig. 7, it can be seen that the CH HDA reduces the HoF ratio effectively when the initial $Offset_n$ is in the interval of less than and more than optimal $Offset_n$ 2.5 dB, which increases the number of handovers while obtaining better performance. In addition, it can also be effective in reducing the number of specific types of HoF, TLFs, or TEFs.

3) EVALUATION OF UE MOVING WITH 3 M/S

Fig. 8 shows the HoF ratio and number of handovers of two HDAs when the T_{CQI_2} is fixed to 2, and the UE moves at 3 m/s.

Fig. 8a shows that the HoF ratio for A3RSRP HDA is 13%. In contrast, the CH HDA reduces the HoF ratio by 2% and no change, respectively, when the T_{CQI_1} is 4 with and without HC, while the CH HDA increases the HoF ratio by 2% and 3%, respectively, when the T_{CQI_1} is 3 with and without HC, respectively, compared with the A3RSRP HDA. Moreover, the number of handovers and TEFs reduces by 18% and 5%, respectively, while the number of TLFs increases by 8% for CH HDA compared to A3RSRP HDA when the T_{CQI_1} 3 without HC based on the result in Fig. 9a. Additionally, the number of handovers and TEFs decreases by 20% and 20%, respectively, while the number of TLFs increases by 8% when the T_{CQI_1} is 3 with HC and the sum of H is -0.5 dB, and the number of handovers and TEFs reduces by 21% and 25% when the T_{CQI_1} is 3 and the sum of H is 0 dB, while the number of TLFs increases by 8%. As mentioned, the reduction in the number of handovers and TEFs and the increase in the number of TLFs is because of the substantial suppression effect of the T_{CQI_1} 3.

Meanwhile, the number of handovers, TLFs, and TEFs are reduced by 6%, 4%, and 40%, respectively, when the T_{CQI_1} is 4 with HC and the sum of H parameters is -0.5 dB. In addition, the number of handovers, TLFs, and TEFs is reduced by 7%, 6%, and 30%, respectively, when the T_{CQI_1} is 4 with HC and the sum of H parameters is 0.0 dB. Although the suppression of handovers and TEFs is degraded when the T_{CQI_1} is 4 compared to the T_{CQI_1} is 3, the improvement by the T_{CQI_1} 4 is better than the T_{CQI_1} 3, because the shifted trigger timing of handover by the HC is more suitable with T_{CQI_1} 4 than with T_{CQI_1} 3 at a moving speed of 3.0 m/s.

Fig. 8b shows that the HoF ratio for the A3RSRP HDA is 14%. In contrast, the HoF ratio of CH HDA is 15% when the T_{CQI_1} is 4 with or without HC, and the HoF ratio of CH HDA is 16% when the T_{CQI_1} is 3 with or without HC compared with the A3RSRP HDA. Moreover, the CH HDA increases the number of handovers, TLFs, and TEFs by 2%, 8%, and 42%, respectively, when the T_{CQI_1} is 3 based on the in Fig. 9b. When T_{CQI_1} is 4, the number of handovers and TEFs does not change, while the number of TLFs increases by 8% compared with the A3RSRP HDA. Because an initial $Offset_n$ value of 1.0 dB is the optimal parameter for A3RSRP HDA with a speed of 3 m/s, and the same reason as in Fig. 6e.

Fig. 8c shows that the HoF ratio for the A3RSRP HDA is 16%. In contrast, the HoF ratio for CH HDA decreases

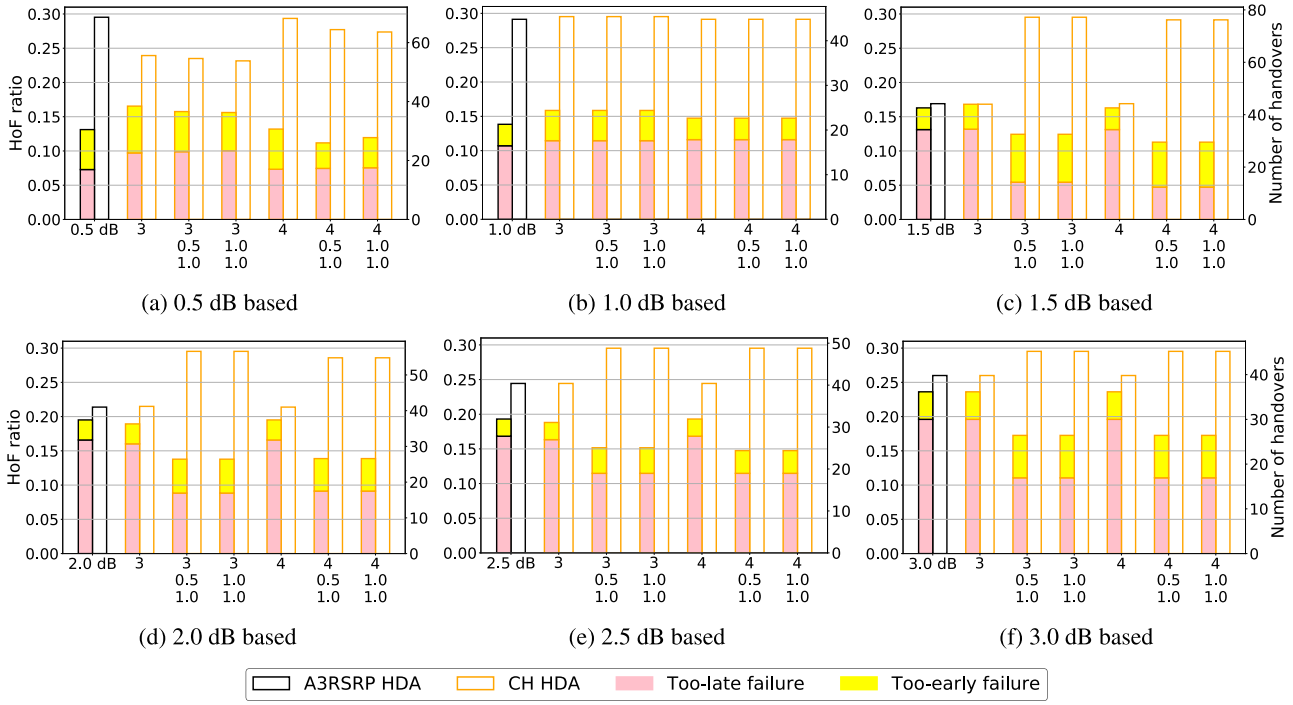

FIGURE 8. Comparison of the HoF ratio and number of handovers for the A3RSRP and CH HDAs at 3 m/s speed.

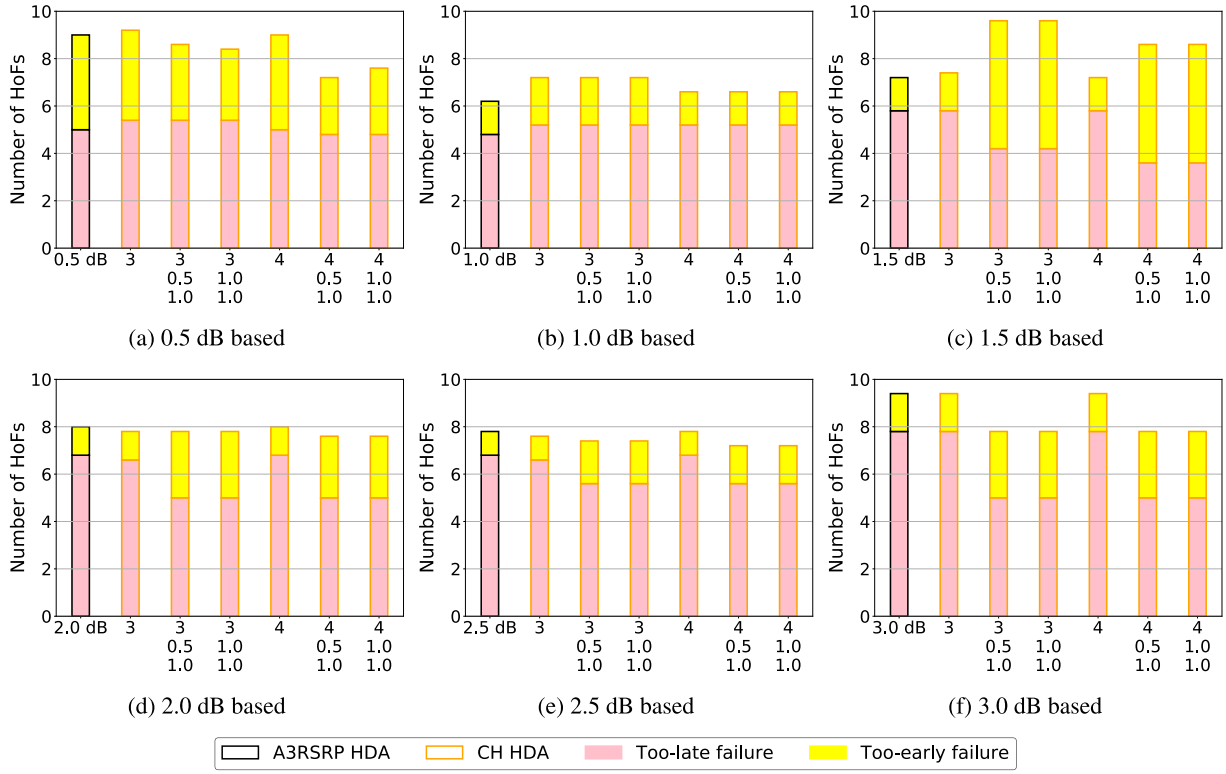

FIGURE 9. Comparison of the number of HoFs for the A3RSRP and CH HDAs at 3 m/s speed.

by 4% when the T_{CQI_1} is 3 with HC, while the HoF ratio increases little when the T_{CQI_1} is 3 without HC compared with the A3RSRP HDA. The HoF ratios remain unchanged when T_{CQI_1} is 4 without HC compared with the A3RSRP HDA. Moreover, the number of TLFs decreases by 27% while the number of handovers and TEFs increase by 74% and 285%,

respectively, when the T_{CQI_1} is 3 with HC, while the number of TEFs remains the same and the number of handovers increases little when T_{CQI_1} is 3 without HC compared with the A3RSRP HDA based on the in Fig. 9c. The reason for the higher increase in the number of TEFs is that in order to reduce the TLFs dominated in the HoFs, the H^- dominates in HC. Thus, the number of handovers and TEFs is increased while the number of TLFs is reduced. Meanwhile, the number of TLFs decreases by 38% while the number of handovers and TEFs increases by 41% and 257%, respectively, when the T_{CQI_1} is 4 with HC, whereas the results are unchanged when the T_{CQI_1} 4 without HC compared with the A3RSRP HDA.

Fig. 8d shows that the HoF ratio for the A3RSRP HDA is 19%. In contrast, the CH HDA decreases the HoF ratio by 5% when T_{CQI_1} is 3 with HC, and the HoF ratio decreases slightly when T_{CQI_1} is 3 without HC compared with the A3RSRP HDA. The HoF rate decreases by 5% when T_{CQI_1} is 4 with HC, and there is no change in the HoF rate when the T_{CQI_1} is 4 without HC. Moreover, the number of TLFs reduces by 2% while the number of handovers increases by 38%, and the number of TEFs remains unchanged when T_{CQI_1} is 3 without HC, and the number of TLFs reduces by 30% while the number of handovers and TEFs increase by 38% and 250%, respectively, when the T_{CQI_1} is 3 with HC compared with the A3RSRP HDA based on the in Fig. 9d. Meanwhile, the number of TLFs reduces by 28% while the number of handovers and TLFs increases by 33% and 200% when T_{CQI_1} is 4 with HC, the number of handovers, TLFs, and TEFs remain unchanged when T_{CQI_1} is 4 without HC compared with the A3RSRP HDA.

Fig. 8e shows that the HoF ratio for the A3RSRP HDA is 19%. In contrast, the HoF ratio for the CH HDA reduces by 4% when T_{CQI_1} is 3 with HC and reduces less when the T_{CQI_1} is 3 without HC. The HoF ratio reduces by 4% when T_{CQI_1} is 4 with HC, while the HoF ratio remains unchanged when T_{CQI_1} is 4 without HC. Moreover, the number of TLFs reduces by 3%, while the number of handovers and TEFs remains the same when T_{CQI_1} is 3 without HC The number of TLFs reduces by 17% while the number of handovers and TEFs increases by 20% and 80%, respectively, when T_{CQI_1} is 3 with HC compared with the A3RSRP HDA based on the in Fig. 9d. Meanwhile, the number of TLFs reduces by 17% while the number of handovers and TEFs increases by 17% and 60%, respectively, when T_{CQI_1} is 4 with HC, and the number of handovers and HoFs is the same when T_{CQI_1} is 4 without HC compared with the A3RSRP HDA.

Fig. 8f shows that the HoF ratio of A3RSRP HDA is 24%. In contrast, the CH HDA reduces the HoF ratio by 6% when T_{CQI_1} are 3 and 4 with HC compared to the A3RSRP HDA, while the HoF ratio of the CH HDA remains unchanged compared to the A3RSRP HDA when T_{CQI_1} are 3 and 4 with no HC. Moreover, the number of TLFs decreases by 37%, while the number of handovers and TEFs increases by 13% and 100%, respectively, and all results remain unchanged when T_{CQI_1} are 3 and 4 without HC based on the result in Fig. 9f.

TABLE 2. Optimal parameters setting for the small-scale environment.

HDA	Speed	$Offset_n$	T_{CQI_1}	T_{CQI_2}	H^+	H^-
A3RSRP	0.5 m/s	3.0 dB	n/a	n/a	n/a	n/a
	1 m/s	2.5 dB	n/a	n/a	n/a	n/a
	3 m/s	1.0 dB	n/a	n/a	n/a	n/a
CH	0.5 m/s	3.0 dB	3	1	n/a	n/a
		3.0 dB	3	1	1.0 dB	0.0 dB
	1 m/s	3.0 dB	3	2	1.0 dB	0.5 dB
		3.0 dB	4	2	1.0 dB	0.5 dB
	3 m/s	1.5 dB	3	2	0.5 dB	1.0 dB
		1.5 dB	4	2	0.5 dB	1.0 dB

Based on the results of the scenario with a speed of 3.0 m/s, the difference compared to the scenario with a moving speed of 1 m/s is that the effect of CH HDA to reduce the HoF ratio is mainly provided by the H^- of 1.0 dB, which is raised by 0.5 dB compared to the scenario with a speed of 1 m/s. This is due to the increase in the ratio of TLFs in HoFs with an increased speed, a higher H^- parameter is required to reduce the difficulty of the handover triggering to reduce the higher ratio of TLFs in HoFs. Simultaneously, the CH HDA reduces the HoF ratio, while the number of TLFs while slightly increasing the absolute number of TEFs. In addition, the same as in the 1 m/s scenario, the optimal parameter $Offset_n$ changes from 2.5 dB to 1.0 dB for the A3RSRP HDA due to the increase of moving speed, while the improvement of the HoF ratio by the CH HDA on the optimal parameter is not desirable.

C. OPTIMAL PARAMETER SETTING ON SMALL SCALE ENVIRONMENT

To achieve the best CH HDA performance in different environments, for example, it is recommended to use a larger H^+ parameter to reduce the number of FHOs and TEFs with the combination of T_{CQI_1} 3 and T_{CQI_2} 1 to reduce the HoF ratio in a low-speed scenario.

Simultaneously, with increasing speed, it is recommended to use a larger H^- parameter to reduce the number of TLFs under the combination of T_{CQI_1} 3 and T_{CQI_2} 2.

Meanwhile, the proposed CH HDA has multiple parameters in addition to $Offset_n$ compared with the A3RSRP HDA, and multiple parameter combinations exist that can enable the CH HDA to show the best performance on the HoF ratio, and there exhibits two settings of optimal parameters for CH HDA in different scenarios.

Therefore, based on the simulation results in Fig. 4, 6, 8, the optimal parameter combinations for the two HDAs in the HetNet environment are shown in Table 2.

D. SIMULATION ENVIRONMENT WITH LARGE SCALE

The large-scale environment is illustrated in Fig. 10. Two macro-cells are placed at (0, 0) and (1000, 0), and five small-cells are placed at (500, 200), (500, 100), (500, 0), (500, −100), and (500, −200). The distance between the small-cells is 100 m. The UEs are randomly placed on the

range of the X-axis [200, 800] and Y-axis [−200, 200]. The simulation parameter settings for the rest of the environment are the same as for the small-scale environment, refer to Table 1.

In the small-scale environment, the optimal parameter setting for the $Offset_n$ was found in the range of (0.5, 3.0) dB. Therefore, in the large-scale environment, the values of the optimal $Offset_n$ (1.0 dB, 2.5 dB, and 3.0 dB) are used to compare the performance of the two HDAs.

However, the co-frequency interference in the large-scale environment is more significant than in the small-scale environment owing to the increased number of cells using the same frequency.

As a result, the increase in interference after more cells using the same frequency leads to a degradation in the CQI of UE at the trigger timing of the handover. Specifically, in the small-scale environment, the value of CQI when the UE triggers a handover is generally 2 or 3. Conversely, the CQI value when the UE triggers a handover in the large-scale environment is generally 1 or 2.

Therefore, to ensure that the CH HDA is able to correctly determine the trigger timing of the handover and the suppression effect on the FHO and TEF even in a large-scale environment with strong interference. We reduce the threshold value of T_{CQI_1} and use 2 and 3 as the T_{CQI_1} parameter and 1 as the T_{CQI_2} parameter in the large-scale environment. The relationship between the number of cells with co-frequency interference and the selection of T_{CQI_1} is not considered in this paper.

In addition, with an increase in the number of cells, the UE receives signals from more co-frequency interference cells, thereby enhancing the effect of multipath propagation in signal propagation, leading to severe fading compared to small-scale environments. Therefore, in the large-scale environment, the HC has a positive effect on the parameter H^+. The performance results for the large-scale environment are shown in Fig. 11, 12, 13 , 14, 15 , and 16, respectively.

1) EVALUATION OF UE MOVING WITH 0.5 M/S

The simulation results are shown in Fig. 11 and Fig. 12 when the UE is moving at 0.5 m/s with the $Offset_n$ is 1.0 dB, 2.5 dB, and 3.0 dB.

Fig. 11a shows that the HoF ratio of A3RSRP HDA is 15%. Moreover, because of the severe fading caused by the inclusion of more cells, a large number of handovers occur despite the UE moving at a very low speed of 0.5 m/s. This occurrence is attributed to the large number of handovers caused by the selection of a smaller $Offset_n$ as a threshold value in the fading environment. This result is the same as that in Fig. 4a.

In contrast, the CH HDA slightly reduced HoF ratios when T_{CQI_1} is 2 with or without HC. Moreover, the number of handovers and TEFs is reduced by 26% and 31%, respectively, while the number of TLFs slightly increases when T_{CQI_1} is 2 with or without HC compared with A3RSRP HDA based on the result in Fig. 12. This is because as with

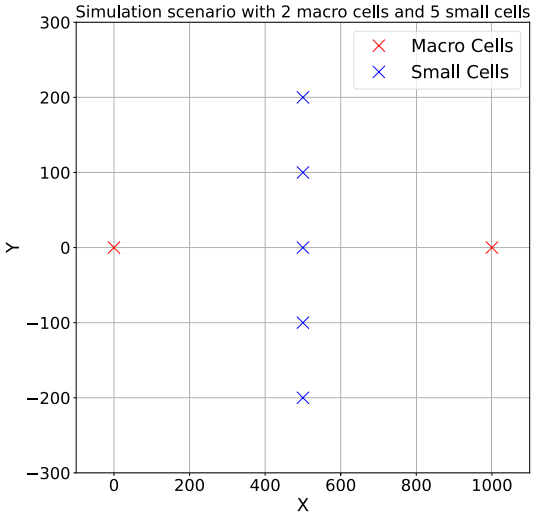

FIGURE 10. Simulation environment with large scale.

T_{CQI_1} 3 in the small-scale environment, T_{CQI_1} 2 suppresses a large number of handovers but it also significantly shifts the timing of handover trigger, resulting in a slight increase in the number of TLFs.

Meanwhile, the CH HDA reduces the HoF ratio by 4% and 3% when T_{CQI_1} is 3 and with or without HC, respectively. Moreover, the number of handovers and TEFs for CH HDA decreases by 17% and 34%, respectively, and the number of TLFs increases slightly compared to A3RSRP HDA when T_{CQI_1} is 3 without HC. For the current scenario with a small initial $Offset_n$, 1.0 dB, the result by the sum of the H of 0.5 dB is better than the sum of 1.0 dB for determining the timing of the handover trigger. This is the same as in Fig. 4b.

Fig. 11b shows that the HoF ratio for the A3RSRP HDA is 13%. In contrast, the CH HDA reduces the HoF ratio by 1% when T_{CQI_1} is 2 with or without HC. Moreover, the number of TLFs reduces by 100% with an absolute zero, and the number of TEFs reduces by 54% when T_{CQI_1} is 2 with or without HC compared with the A3RSRP HDA. The number of handovers, TLFs, and TEFs reduces by 43%, 100%, and 44%, respectively, while the HoF ratio does not change when T_{CQI_1} is 3 without HC, while the number of handovers, TLFs, and TEFs reduces by 44%, 100%, and 53%, respectively, when HC is considered with the sum of the H 1.0 dB compared with the A3RSRP HDA based on the result in Fig. 12b. Compared to the result in the small-scale environment, the reduction of the HoF ratio by CH HDA is smaller compared with the A3RSRP HDA because the CH HDA suppresses a large number of FHOs. Therefore, although the improvement in the HoF ratio is slightly smaller for the CH HDA, the effect of the CH HDA in reducing FHO and HoFs is substantial.

Fig. 11c shows that the HoF ratio of the A3RSRP HDA is 12%. In contrast, the HoF ratio of the CH HDA increases by 4% and 1% compared with the A3RSRP HDA when T_{CQI_1} is 2 and 3, respectively. Moreover, the number of handovers

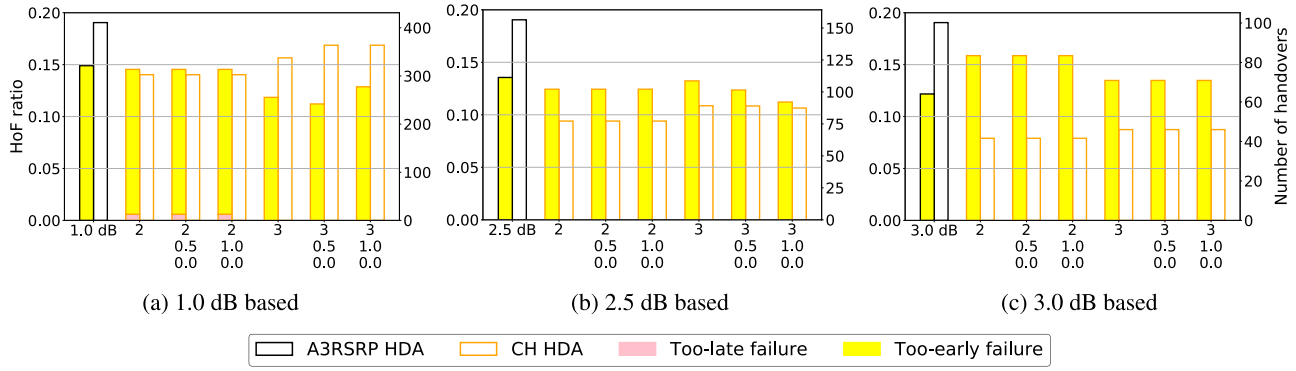

FIGURE 11. Comparison of HoF ratio and number of handovers for the A3RSRP and CH HDAs at 0.5 m/s speed.

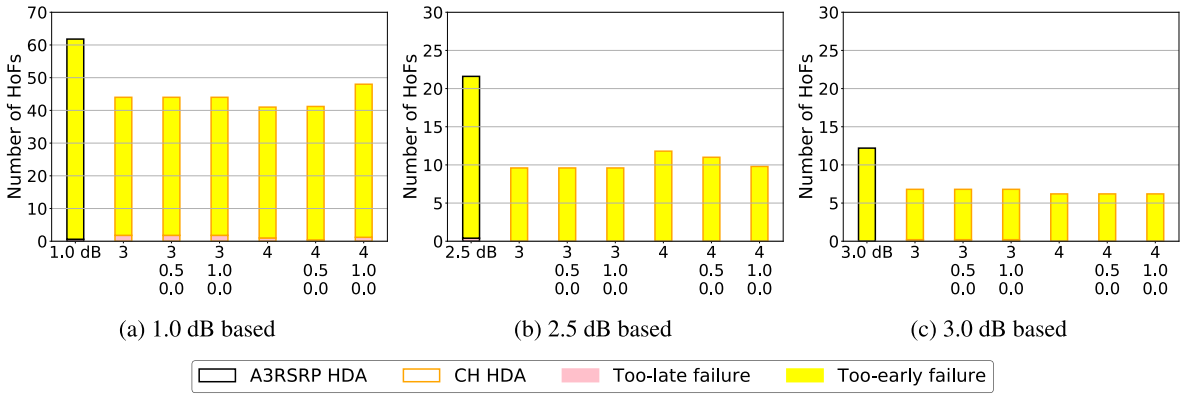

FIGURE 12. Comparison of number of HoFs for the A3RSRP and CH HDAs at 0.5 m/s speed.

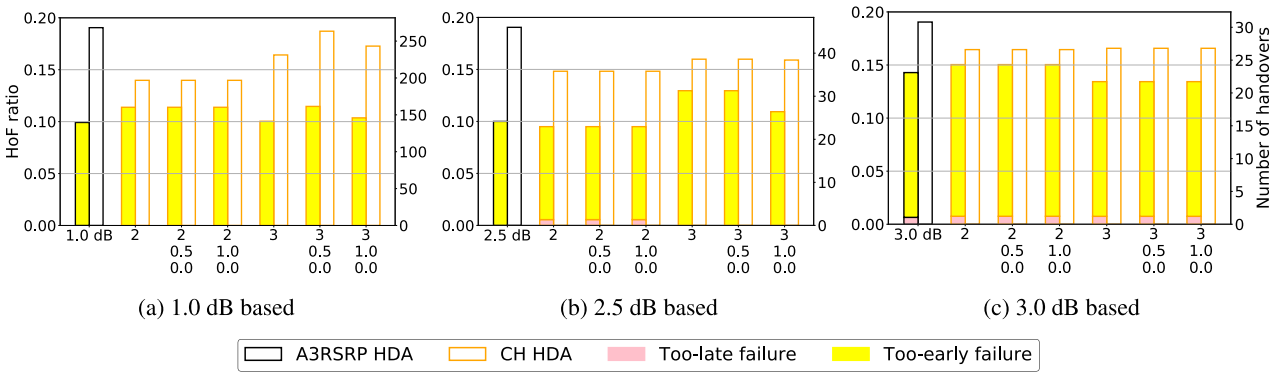

FIGURE 13. Comparison of HoF ratio and number of handovers for the A3RSRP and CH HDAs at 1 m/s speed.

reduces by 58% and 54%, and the number of TELs reduces by 46% and 49%, respectively, while a small increase in the number of TLFs occurs when T_{CQI_1} is 2 based on the result in Fig. 12c.

2) EVALUATION OF UE MOVING WITH 1.0 M/S

The simulation results when the moving speed of UE is 1.0 m/s, and $Offset_n$ is 1.0 dB, 2.5 dB, and 3.0 dB are shown in Fig. 13 and Fig. 14.

Fig. 13a shows that the HoF ratio increased by 1% with the T_{CQI_1} of 2 and with and without HC compared with A3RSRP HDA. Nevertheless, the number of handovers and TEFs reduced by 26% and 15%, respectively, while the number of TLFs reduced slightly compared with A3RSRP HDA based on the result in Fig. 14a. Meanwhile, the HoF ratio does not change when T_{CQI_1} is 3 and without HC compared with A3RSRP HDA. The number of handovers and TEFs reduced by 13% and 12%, respectively, while the number of TLFs increased slightly compared with A3RSRP HDA. The number of handovers reduces by 1% and 9% compared to A3RSRP HDA when T_{CQI_1} is 3 with HC, respectively, while the number of TEFs increases by 13% when the sum of H is 0.5 dB and it for the same reason as the results in Fig. 6b.

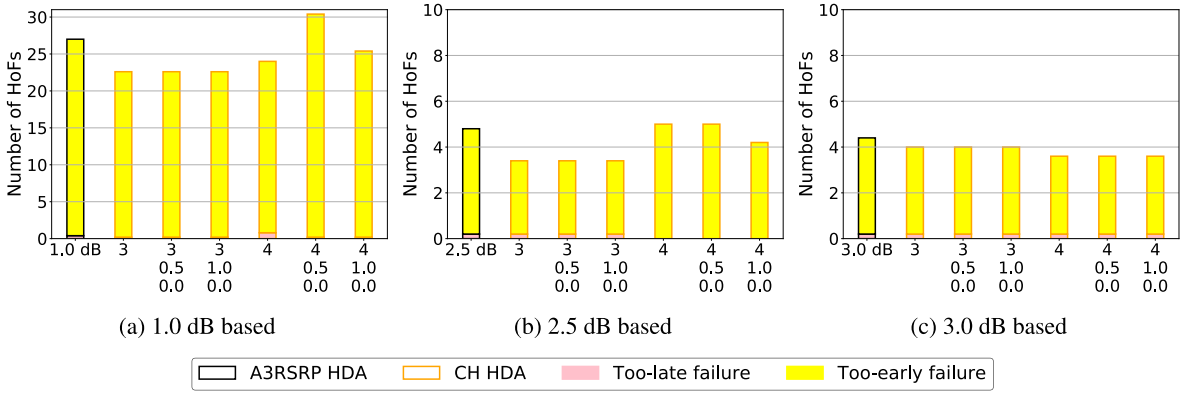

FIGURE 14. Comparison of number of HoFs for the A3RSRP and CH HDAs at 1 m/s speed.

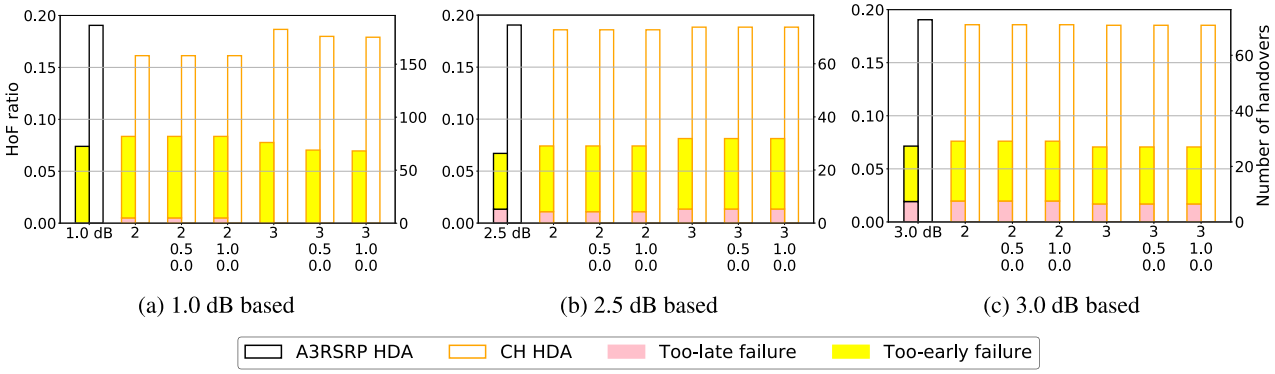

FIGURE 15. Comparison of HoF ratio and number of handovers for the A3RSRP and CH HDAs at 3 m/s speed.

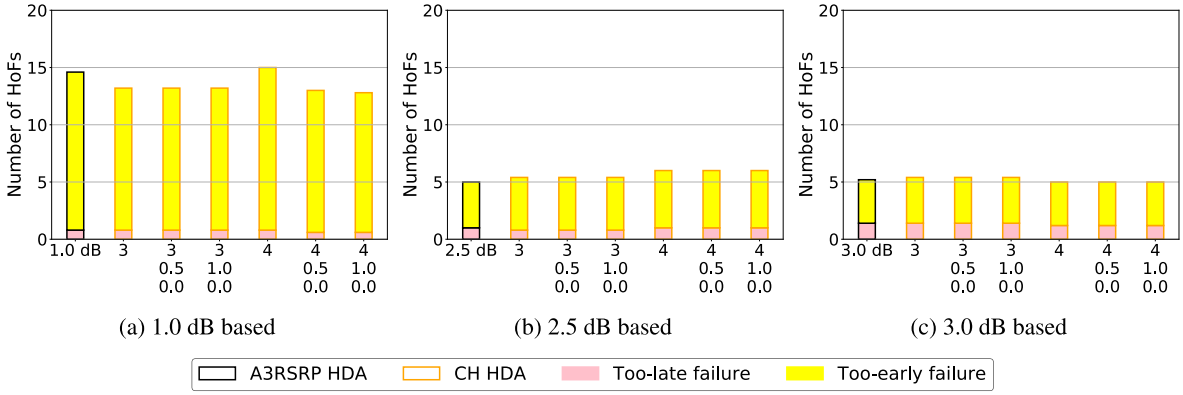

FIGURE 16. Comparison of number of HoFs for the A3RSRP and CH HDAs at 3 m/s speed.

Fig. 13b shows that the HoF ratio for the CH HDA is reduced by 1% with a T_{CQI_1} of 2 and with and without HC, while the HoF ratio for the CH HDA is increased by 2% with a T_{CQI_1} of 3, compared with the A3RSRP HDA. Moreover, the number of handovers and TEFs is reduced by 22% and 30%, respectively, while the number of TLFs is unchanged at a T_{CQI_1} of 2 compared with A3RSRP HDA based on the result in Fig. 14b. At the T_{CQI_1} of 3 and the sum of H of 1.0 dB, the number of handovers and TEFs reduces by 16% and 8%, respectively, while the number of handovers reduces by 16% and the number of TEFs increases by 8% at a sum of H of 0.5 dB, and the reason for this is the same as in Fig. 6e.

Fig. 13c shows that the HoF ratio of CH HDA reduces by 1% when the T_{CQI_1} is 3, while the HoF ratio increases by 1% when the T_{CQI_1} is 2 compared with A3RSRP HDA. Moreover, the number of handovers and TEFs is reduced by 13% and 9%, respectively, when the T_{CQI_1} is 2 compared to A3RSRP HDA, and the number of handovers and TEFs is reduced by

13% and 19%, respectively, when the T_{CQI_1} is 3, while the number of TLFs remains unchanged based on the result in Fig. 14c.

3) EVALUATION OF UE MOVING WITH 3.0 M/S

The simulation results show that the moving speed of UE is 3.0 m/s, and $Offset_n$ of 1.0 dB, 2.5 dB, and 3.0 dB are shown in Fig. 15 and Fig. 16.

Fig. 15 and Fig. 16 show that the HoF ratios of the two HDAs are almost the same. The CH HDA still has a significant effect on reducing the number of handovers compared with the A3RSRP HDA.

Based on the results shown in Fig. 11, 12, 13 , 14, 15, and 16, it can be observed that the HoF ratio in the large-scale environment is lower than the HoF ratio in the small-scale environment, because the increased number of cells that enhances the effect of fading, which results in significantly larger number of handovers than in the small-scale environment, and most of these handovers is the FHO, i.e., unnecessary handovers. Furthermore, the HoF ratios are lower when the UE is moving at 1 m/s and 3 m/s than when the movement speed is 0.5 m/s because handover demand increases with moving speed. This observation is the same as that described in [15] and [33], i.e., UEs moving at low speed are more severely subjected to the fading and experience more TEFs.

Moreover, it is recommended to prioritize the HDA with fewer handovers when the difference in the HoF ratio between two HDAs is less than 2%. Because the HDA with fewer handovers is more stable in performance, it enables a more stable communication environment for the UE.

VI. DISCUSSION

In this section, first, we discuss the optimal parameters regarding the two HDAs in different speed scenarios in a small-scale environment. As well as the HoF ratio and trade-off of handover frequency. Finally, the effect of CH HDA on suppressing the handover triggering and TEF is explained through a case study by using variations of both RSRP and CQI.

A. TRADE-OFF BETWEEN THE HOF RATIO AND HANDOVER FREQUENCY

In the context of handover research, examining the HoF measure is crucial to evaluate the advantages and disadvantages of an algorithm. The HoF ratio calculated by (1) objectively assesses whether the number of HoFs in an HDA is low and whether an HDA is usable.

Unfortunately, a single performance measure, such as the HoF ratio, is not sufficient to completely evaluate an HDA. For example, if the conditions for determining the handover trigger by a HDA are excessively relaxed, such as the results for the A3RSRP HDA in Fig. 4 and Fig. 11, it results in a large number of handovers, the FHO, and the HoF ratio will be a small value, as calculated using (1). Especially for a low-speed UE of 0.5 m/s, frequent handovers within a short period pose significant risks.

Therefore, the evaluation of the trade-off between the HoF ratio and handover frequency is another important work to evaluate the merits and drawbacks of an HDA. In this paper, the measure of handover frequency is based on the formula in [32], as follows:

$$HF_{freq} = \frac{N_{\text{ho}}}{N_{user} \times T_{sim}}, \tag{3}$$

where HF_{freq} represents the handover frequency, which indicates the number of handovers per second for each UE. Thus, a higher number indicates a greater frequency of handover for a UE. N_{ho} denotes the number of all handovers, N_{user} denotes the number of UEs, and T_{sim} denotes the simulation time. Using the handover frequency from (3) and the HoF from (1), the trade-off between the HoF ratio and the handover frequency can be evaluated for an HDA.

Fig. 17a shows that the CH HDA has a lower handover frequency than the A3RSRP HDA for all parameter combinations, which is a crucial result for UE moving at low speed because a UE moving at a low-speed has an extremely low requirement for handover and a high handover frequency will result in a severely unstable communication environment. Meanwhile, the CH HDA takes the result of the zero HoF as described in Fig. 4d, hence, the CH HDA has more zero points at the origin than the A3RSRP HDA, and the overall performance is better than the A3RSRP HDA.

Fig. 17b shows that the CH HDA can achieve a lower HoF ratio and handover frequency compared with the A3RSRP HDA. However, the CH HDA has a higher handover frequency than the A3RSRP HDA for certain parameter combinations in order to reduce the HoF ratio.

Fig. 17c shows that the CH HDA has a lower HoF ratio while slightly increasing the frequency of handovers when the CH HDA reduces the HoF ratio and the number of TLFs.

B. A CASE STUDY OF THE SUPPRESSING EFFECTS OF CH HDA ON HANDOVER AND TEF

In Fig. 18, there are three subfigures representing, from top to bottom: the changes in RSRP of the three cells received by the UE during the simulation time 1000 s, the changes in RSRP of the surrounding three cells for 100 ms before and after the handover trigger timing of 438.3 s, and the changes in downlink CQI for 100 ms before and after the handover trigger timing of 438.3 s. The sub-figure on top shows that the UE receives RSRP from three cells that are undergoing fading and changing drastically. The middle subplot indicates that the UE has satisfied the trigger condition for handover by the $Offset_n$ value of 2.0 dB based on (1) at 438.2 s, and the handover from macro-cell to small-cell 2 is triggered at 438.3 s after a TTT of 100 ms. However, the RSRP received by the UE from the macro-cell is again greater than the RSRP received from the small-cell 2 at 438.4 s, 100 ms after the handover is triggered due to the fading, which causes a TEF to occur.

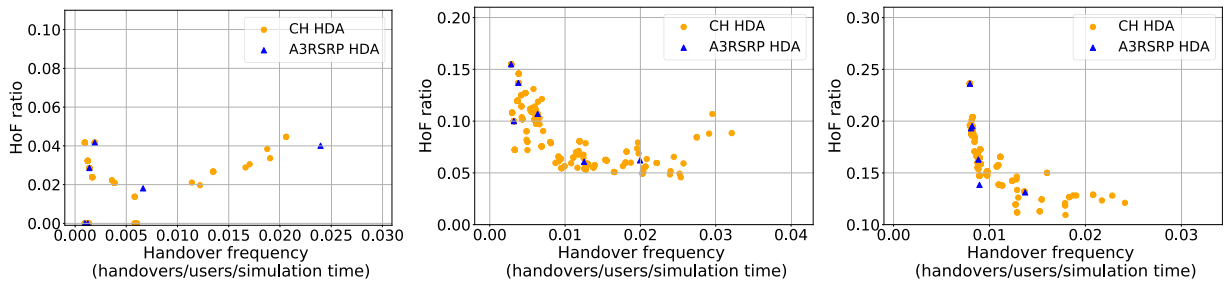

(a) 0.5 m/s-based (b) 1.0 m/s-based (c) 3.0 m/s-based

FIGURE 17. Trade-off between HoF ratio and handover frequency by two HDAs.

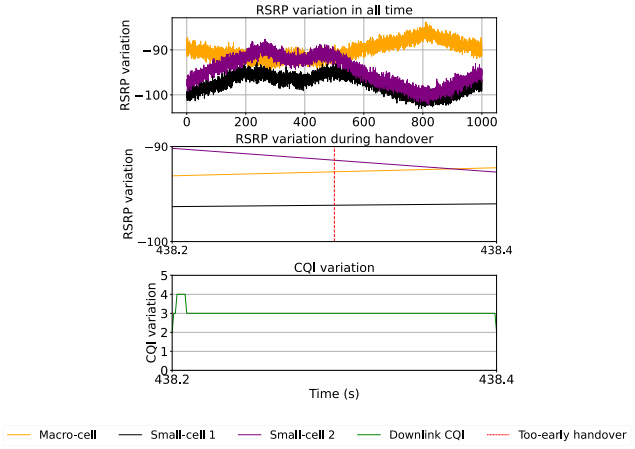

FIGURE 18. The CQI and RSRP variation during a simulation.

On the other hand, for the CH HDA and when the T_{CQI_1} is 3, it can be seen that the CQI of the UE is not less than 3 during the 200 ms period from 438.2 s to 438.4 s. Therefore, the CH HDA can prevent the occurrence of the handover, TEF, and reduce the handover of the UE based on the handover trigger condition of the CH HDA in Algorithm 1. Furthermore, note that not all TEFs can be solved by increasing the TTT because the effect of the fading is difficult to predict, and increasing the TTT may lead to a substantial increase in the number of TLFs and a high HoF ratio. Consequently, the CH HDA shows a substantial effect in suppressing the number of handovers and the number of TEFs based on such a case study in Fig. 18.

VII. CONCLUSION AND FUTURE WORK

In this paper, we propose a novel CQI and HC-based HDA, CH HDA, that prioritizes improving the HoF ratio, followed by the number of handovers and HoFs by shifting the timing of the handover trigger using downlink CQI and HC.

Based on ns-3 simulations, a lower HoF ratio, as well as a lower number of handovers and HoFs, can be achieved using CH HDA compared to the existing A3RSRP HDA. Hence, we show the effectiveness of the proposed CH HDA in achieving the objectives.

Specifically, the proposed CH HDA has a lower number of handovers and HoFs than the A3RSRP HDA and achieves the result of zero HoF ratio at a low speed of 0.5 m/s scenario in the small-scale environment, which indicates that the HoFs can be effectively prevented using the proposed CH HDA, enabling a 100% success rate of handover for the UE moving at low-speed. Meanwhile, the CH HDA is effective in reducing the HoF ratio and the number of HoFs at 1 m/s and 3 m/s, which effectively reduces the higher TLF ratio in the HoF ratio, while the number of handover and a few TEFs are increased. Moreover, the proposed CH HDA reduces a significant number of handovers and HoFs compared with the A3RSRP HDA at 0.5 m/s, 1 m/s, and 3 m/s in the large-scale environment, hence the improvement in HoF ratio is not as efficient as in the small-scale environment.

Therefore, the CH HDA shows a maximum improvement of 100% in HoF ratio and 5% and 100% in handover and number of HoFs, respectively, compared with the A3RSRP HDA in the small-scale environment with a speed of 0.5 m/s and an initial $Offset_n$ of 2.0 dB. In contrast, CH HDA shows a minimum improvement of -4% in HoF ratio and 58% and 44% improvement in handover and number of HoFs, respectively, compared with the A3RSRP HDA in the large-scale environment with a speed of 0.5 m/s and an initial $Offset_n$ of 3.0 dB.

Finally, at the end of the paper, we further discuss the trade-off between the proposed CH and A3RSRP HDA in terms of the HoF ratio and handover frequency, as well as explain the specific actions of CH HDA in reducing the HoF ratio, the number of handovers, and the number of HoFs by a case study. The trade-off results show that the proposed CH HDA shows better performance than the A3RSRP HDA in both HoF ratio and handover frequency in the scenarios of 0.5 m/s, 1 m/s, and 3 m/s, whereas it is worse than the A3RSRP HDA in terms of handover frequency in the scenario of 3 m/s. In the case study, we explain the effectiveness of the CH HDA in suppressing the handover and HoF.

In future work, we will investigate a method that reduces both HoFs (TLF and TEF) simultaneously, even in a high-speed scenario, and use it in the CH HDA. It may be necessary to assume a specific movement and observe

the fading-induced changes in CQI and RSRP to estimate accurately the successful timing of the handover trigger to improve our HDA. In addition, the changes in interference strength caused by the different numbers of co-frequency cells lead to variations in the parameters setting for the CH HDA. Therefore, we will discuss the relationship between the parameters setting of the CH HDA and the number of co-frequency cells in HetNet to further improve the robustness of our CH HDA in different HetNet environments. Moreover, since the proposed CH HDA has a lower HoF ratio and the number of handovers and HoFs, the proposed CH HDA does not need to consume a lot of computation time and resources. Thus, the CH HDA has the potential to be applied to real LTE or 5G scenarios to improve the high handover latency and low throughput due to the high HoF ratio and provide a better user experience.

REFERENCES

[1] D. Castro-Hernandez and R. Paranjape, "Optimization of handover parameters for LTE/LTE-A in-building systems," *IEEE Trans. Veh. Technol.*, vol. 67, no. 6, pp. 5260–5273, Jun. 2018.
[2] M. M. Hasan, S. Kwon, and J.-H. Na, "Adaptive mobility load balancing algorithm for LTE small-cell networks," *IEEE Trans. Wireless Commun.*, vol. 17, no. 4, pp. 2205–2217, Apr. 2018.
[3] S. Nayak, "ns-3 simulation based exploration of LTE handover optimization," *EAI Endorsed Trans. Mobile Commun. Appl.*, vol. 7, no. 4, p. e4, May 2023.
[4] T. A. Achhab, F. Abboud, and A. Assalem, "A robust self-optimization algorithm based on idiosyncratic adaptation of handover parameters for mobility management in LTE-A heterogeneous networks," *IEEE Access*, vol. 9, pp. 154237–154264, 2021.
[5] D. Xenakis, N. Passas, L. Merakos, and C. Verikoukis, "Mobility management for femtocells in LTE-advanced: Key aspects and survey of handover decision algorithms," *IEEE Commun. Surveys Tuts.*, vol. 16, no. 1, pp. 64–91, 1st Quart., 2014.
[6] Y.-H. Wang, J.-L. Chang, and G.-R. Huang, "A handover prediction mechanism based on LTE-A UE history information," in *Proc. 18th Int. Conf. Netw.-Based Inf. Syst.*, Sep. 2015, pp. 167–172.
[7] A. U. Rehman, M. B. Roslee, and T. Jun Jiat, "A survey of handover management in mobile HetNets: Current challenges and future directions," *Appl. Sci.*, vol. 13, no. 5, p. 3367, Mar. 2023.
[8] H. Park, Y. Lee, T. Kim, B. Kim, and J. Lee, "ZEUS: Handover algorithm for 5G to achieve zero handover failure," *ETRI J.*, vol. 44, no. 3, pp. 361–378, Jun. 2022.
[9] H.-S. Park, Y. Lee, T.-J. Kim, B.-C. Kim, and J.-Y. Lee, "Faster recovery from radio link failure during handover," *IEEE Commun. Lett.*, vol. 24, no. 8, pp. 1835–1839, Aug. 2020.
[10] W. Zheng, H. Zhang, X. Chu, and X. Wen, "Mobility robustness optimization in self-organizing LTE femtocell networks," *EURASIP J. Wireless Commun. Netw.*, vol. 2013, no. 1, pp. 1–10, Feb. 2013.
[11] K. Kitagawa, T. Komine, T. Yamamoto, and S. Konishi, "A handover optimization algorithm with mobility robustness for LTE systems," in *Proc. IEEE 22nd Int. Symp. Pers., Indoor Mobile Radio Commun.*, Toronto, ON, Canada, Sep. 2011, pp. 1647–1651.
[12] A. Madelkhanova, Z. Becvar, and T. Spyropoulos, "Optimization of cell individual offset for handover of flying base stations and users," *IEEE Trans. Wireless Commun.*, vol. 22, no. 5, pp. 3180–3193, May 2023.
[13] Y. Song, S. H. Lim, and S.-W. Jeon, "Handover decision making for dense HetNets: A reinforcement learning approach," *IEEE Access*, vol. 11, pp. 24737–24751, 2023.
[14] Y. Ullah, M. B. Roslee, S. M. Mitani, S. A. Khan, and M. H. Jusoh, "A survey on handover and mobility management in 5G HetNets: Current state, challenges, and future directions," *Sensors*, vol. 23, no. 11, p. 5081, May 2023.
[15] W. Tashan, I. Shayea, S. Aldirmaz-Colak, M. Ergen, M. H. Azmi, and A. Alhammadi, "Mobility robustness optimization in future mobile heterogeneous networks: A survey," *IEEE Access*, vol. 10, pp. 45522–45541, 2022.
[16] S. Nie, D. Wu, M. Zhao, X. Gu, L. Zhang, and L. Lu, "An enhanced mobility state estimation based handover optimization algorithm in LTE-A self-organizing network," *Proc. Comput. Sci.*, vol. 52, pp. 270–277, Jan. 2015.
[17] I. Shayea, M. Ergen, A. Azizan, M. Ismail, and Y. I. Daradkeh, "Individualistic dynamic handover parameter self-optimization algorithm for 5G networks based on automatic weight function," *IEEE Access*, vol. 8, pp. 214392–214412, 2020.
[18] F. Afroz, R. Subramanian, R. Heidary, K. Sandrasegaran, and S. Ahmed, "SINR, RSRP, RSSI and RSRQ measurements in long term evolution," *Int. J. Wireless Mobile Netw.*, vol. 7, no. 4, pp. 1–12, Aug. 2015.
[19] S. Winder, "Buck-based LED drivers," in *Power Supplies for LED Driving*, 2nd ed. Oxford, U.K.: Newnes, 2017, ch. 5, pp. 43–71.
[20] M. M. Hasan, S. Kwon, and S. Oh, "Frequent-handover mitigation in ultra-dense heterogeneous networks," *IEEE Trans. Veh. Technol.*, vol. 68, no. 1, pp. 1035–1040, Jan. 2019.
[21] *Self-Organising Networks (SON): Concepts and Requirements*, document 3GPP TS 32.500, Version 0.5.1, Release 8, 2008.
[22] U. Mahamod, H. Mohamad, I. Shayea, M. Othman, and F. A. Asuhaimi, "Handover parameter for self-optimisation in 6G mobile networks: A survey," *Alexandria Eng. J.*, vol. 78, pp. 104–119, Sep. 2023.
[23] M. T. Nguyen, S. Kwon, and H. Kim, "Mobility robustness optimization for handover failure reduction in LTE small-cell networks," *IEEE Trans. Veh. Technol.*, vol. 67, no. 5, pp. 4672–4676, May 2018.
[24] A. Alhammadi, W. H. Hassan, A. A. El-Saleh, I. Shayea, H. Mohamad, and Y. Ibrahim Daradkeh, "Conflict resolution strategy in handover management for 4G and 5G networks," *Comput., Mater. Continua*, vol. 72, no. 3, pp. 5215–5232, 2022.
[25] S. Alraih, R. Nordin, A. Abu-Samah, I. Shayea, N. F. Abdullah, and A. Alhammadi, "Robust handover optimization technique with fuzzy logic controller for beyond 5G mobile networks," *Sensors*, vol. 22, no. 16, Aug. 2022, Art. no. 6199.
[26] V. O. Nyangaresi and A. J. Rodrigues, "Efficient handover protocol for 5G and beyond networks," *Comput. Secur.*, vol. 113, Feb. 2022, Art. no. 102546.
[27] M.-T. Nguyen and S. Kwon, "Machine learning–based mobility robustness optimization under dynamic cellular networks," *IEEE Access*, vol. 9, pp. 77830–77844, 2021.
[28] A. Abdelmohsen, M. Abdelwahab, M. Adel, M. S. Darweesh, and H. Mostafa, "LTE handover parameters optimization using Q-learning technique," in *Proc. IEEE 61st Int. Midwest Symp. Circuits Syst. (MWSCAS)*, Windsor, ON, Canada, Aug. 2018, pp. 194–197.
[29] D. D. S. Souza, R. F. Vieira, M. C. D. R. Seruffo, and D. L. Cardoso, "A novel heuristic for handover priority in mobile heterogeneous networks," *IEEE Access*, vol. 8, pp. 4043–4050, 2020.
[30] F. Guidolin, I. Pappalardo, A. Zanella, and M. Zorzi, "Context-aware handover policies in HetNets," *IEEE Trans. Wireless Commun.*, vol. 15, no. 3, pp. 1895–1906, Mar. 2016.
[31] M. I. Goh, A. I. Mbulwa, H. T. Yew, A. Kiring, S. K. Chung, A. Farzamnia, A. Chekima, and M. K. Haldar, "Handover decision-making algorithm for 5G heterogeneous networks," *Electronics*, vol. 12, no. 11, p. 2384, May 2023.
[32] X. Gelabert, G. Zhou, and P. Legg, "Mobility performance and suitability of macro cell power-off in LTE dense small cell HetNets," in *Proc. IEEE 18th Int. Workshop Comput. Aided Modeling Design Commun. Links Netw. (CAMAD)*, Berlin, Germany, Sep. 2013, pp. 99–103.
[33] A. Alhammadi, M. Roslee, M. Y. Alias, I. Shayea, S. Alraih, and K. S. Mohamed, "Auto tuning self-optimization algorithm for mobility management in LTE-A and 5G HetNets," *IEEE Access*, vol. 8, pp. 294–304, 2020.

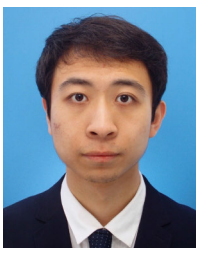

ZHIYI ZHU (Student Member, IEEE) was born in Handan, China, in 1995. He received the Chinese B.E. degree in information technology from Shaoxing University, in 2017, and the M.E. degree from Ritsumeikan University, Japan, in 2021. He is currently pursuing the Ph.D. degree with Kobe University, Japan. His research interests include handover optimization and modeling analysis of handover. He is a Student Member of IEEE Computer Society and IEEE Reliability.

EIJI TAKIMOTO was born in Shizuoka, Japan, in 1976. He received the B.E., M.E., and Ph.D. degrees in computer science from Ritsumeikan University, Japan, in 1998, 2000, and 2015, respectively. He has been an Associate Professor with Nara Woman's University, since 2022. His current research interests include computer security and computer networks. He is a member of the Information Processing Society of Japan (IPSJ), the Institute of Electronics, Information and Communication Engineers (IEICE), and the Institute of Systems, Control, and Information Engineers (ISCIE), Japan.

PATRICK FINNERTY (Member, IEEE) was born in Cholet, France, in 1995. He received the French Engineering degree in computer science and information technology from INSA Lyon, in 2018, and the Ph.D. (Eng.) degree from Kobe University, Japan, in 2022. Since February 2022, he has been an Assistant Professor with the Graduate School of System Informatics, Kobe University. His research interests include parallel and distributed computing techniques and distributed systems. He is a member of IPSJ, IEEE Computer Society, and ACM.

CHIKARA OHTA (Member, IEEE) was born in Osaka, Japan, in 1967. He received the B.E., M.E., and Ph.D. (Eng.) degrees in communication engineering from Osaka University, Osaka, in 1990, 1992, and 1995, respectively. In April 1995, he was an Assistant Professor with the Department of Computer Science, Faculty of Engineering, Gunma University. In October 1996, he was a Lecturer with the Department of Information Science and Intelligent Systems, Faculty of Engineering, University of Tokushima, and an Associate Professor, in March 2001. In November 2002, he was an Associate Professor with the Department of Computer and Systems Engineering, Faculty of Engineering, Kobe University. In April 2010, he was an Associate Professor with the Graduate School of System Informatics, Kobe University, and a Professor, in January 2015. In April 2016, he was a Professor with the Graduate School of Science, Technology and Innovation, Kobe University. Since April 2022, he has been a Professor with the Graduate School of System Informatics, Kobe University. From March 2003 to February 2004, he was a Visiting Scholar with the University of Massachusetts at Amherst, USA. His current research interest includes the performance evaluation of communication networks. He is a member of IPSJ and ACM SIGCOMM.